Title

Importance of titanohematite in detrital remanent magnetizations of strata spanning the Cretaceous-Paleogene boundary, Hell Creek region, Montana

Journal

Geochemistry Geophysics Geosystems, 17(3)

ISSN

1525-2027

Authors

Sprain, Courtney J
Feinberg, Joshua M
Renne, Paul R
et al.

Publication Date

2016-03-01

DOI

10.1002/2015gc006191

Peer reviewed

AGU PUBLICATIONS

Geochemistry, Geophysics, Geosystems

RESEARCH ARTICLE
10.1002/2015GC006191

Special Section:
Magnetism From Atomic to Planetary Scales: Physical Principles and Interdisciplinary Applications in Geo- and Planetary Sciences

Importance of titanohematite in detrital remanent magnetizations of strata spanning the Cretaceous-Paleogene boundary, Hell Creek region, Montana

Courtney J. Sprain[1,2], Joshua M. Feinberg[3,4], Paul R. Renne[1,2], and Mike Jackson[3,4]

[1]Department of Earth and Planetary Science, University of California, Berkeley, California, USA, [2]Berkeley Geochronology Center, Berkeley, California, USA, [3]Department of Earth Sciences, University of Minnesota, Minneapolis, Minnesota, USA, [4]Institute for Rock Magnetism, University of Minnesota, Minneapolis, Minnesota, USA

Key Points:
- Intermediate titanohematite (TH) carries significant remanence in KPg sediments, Hell Creek, MT
- A new self-reversal test provides a unique identifier of TH while quantifying its remanence
- Magnetic similarities between our study and clastics within other Laramide basins imply TH more abundant than thought

Correspondence to:
C. Sprain,
spra0111@berkeley.edu

Citation:
Sprain, C. J., J. M. Feinberg, P. R. Renne, and M. Jackson (2016), Importance of titanohematite in detrital remanent magnetizations of strata spanning the Cretaceous-Paleogene boundary, Hell Creek region, Montana, *Geochem. Geophys. Geosyst.*, *17*, 660–678, doi:10.1002/2015GC006191.

Received 19 NOV 2015
Accepted 29 JAN 2016
Accepted article online 5 FEB 2016
Published online 7 MAR 2016

Abstract Intermediate composition titanohematite, $Fe_{2-y}Ti_yO_3$ with $0.5 \leq y \leq 0.7$, is seldom the focus of paleomagnetic study and is commonly believed to be rare in nature. While largely overlooked in magnetostratigraphic studies, intermediate titanohematite has been identified as the dominant ferrimagnetic mineral in an array of Late Mesozoic and early Cenozoic Laramide clastic deposits throughout the central United States. Intermediate titanohematite is ferrimagnetic and has similar magnetic properties to titanomagnetite, except its unique self-reversing property. Due to these similarities, and with detrital remanent magnetizations masking its self-reversing nature, intermediate titanohematite is often misidentified in sedimentary deposits. Past studies relied upon nonmagnetic techniques including X-ray diffraction and electron microprobe analysis. While these techniques can identify the presence of intermediate titanohematite, they fail to test whether the mineral is the primary recorder. To facilitate the identification of intermediate titanohematite in sedimentary deposits, we characterize this mineral using low-temperature magnetometry and high-temperature susceptibility experiments, and present a new identification technique based on titanohematite's self-reversing property, for sediments that span the Cretaceous-Paleogene boundary (Hell Creek region, Montana). Results from the self-reversal test indicate that the majority of remanence is held by minerals that become magnetized parallel to an applied field, but that intermediate, self-reversing titanohematite ($y = 0.53$–0.63) is an important ancillary carrier of remanence. While earlier literature suggests that intermediate titanohematite is rare in nature, reanalysis using specialized rock magnetic techniques may reveal that it is more abundant in the rock record, particularly within depositional basins adjacent to calc-alkaline volcanics, than previously thought.

1. Introduction

Intermediate composition titanohematite is often described as occurring only rarely in nature. Its paragenesis is restricted to limited geologic environments and it has been documented in few paleomagnetic studies, most commonly by the presence of its unique self-reversing property. Intermediate titanohematite received much interest after *Nagata et al.*'s [1951] discovery of a reversed thermoremanent magnetization (RTRM) in the Haruna dacite tuff from Japan, which complicated early recognition of geomagnetic polarity reversals [*Cox et al.*, 1963; *McDougall and Tarling*, 1963]. Since that time, intermediate titanohematite has been identified only in a handful of other locations, most involving rapidly cooled intermediate calc-alkaline volcanic rocks [*Kennedy*, 1981; *Heller et al.*, 1986; *Lawson et al.*, 1987; *Ozima et al.*, 1992]. Aside from rock magnetic studies of self-reversal mechanisms, intermediate titanohematite is often viewed as a magnetic rarity of negligible importance to most paleomagnetic studies. While this belief prevails, intermediate titanohematite has been identified as the dominant ferrimagnetic mineral in a vast array of Late Mesozoic and early Cenozoic clastic sediments deposited across central North America [e.g., *Force et al.*, 2001], suggesting that it may be more abundant and perhaps more important to paleomagnetic records than previously perceived.

Titanohematite was first identified in clastic sediments by *Butler and Lindsay* [1985] in the Fruitland and Kirtland Formations, the Ojo Alamo Sandstone, and the Nacimiento Formation, which span the Cretaceous-Paleogene boundary in the San Juan basin, New Mexico. Initial paleomagnetic studies [*Taylor and Butler*, 1980;

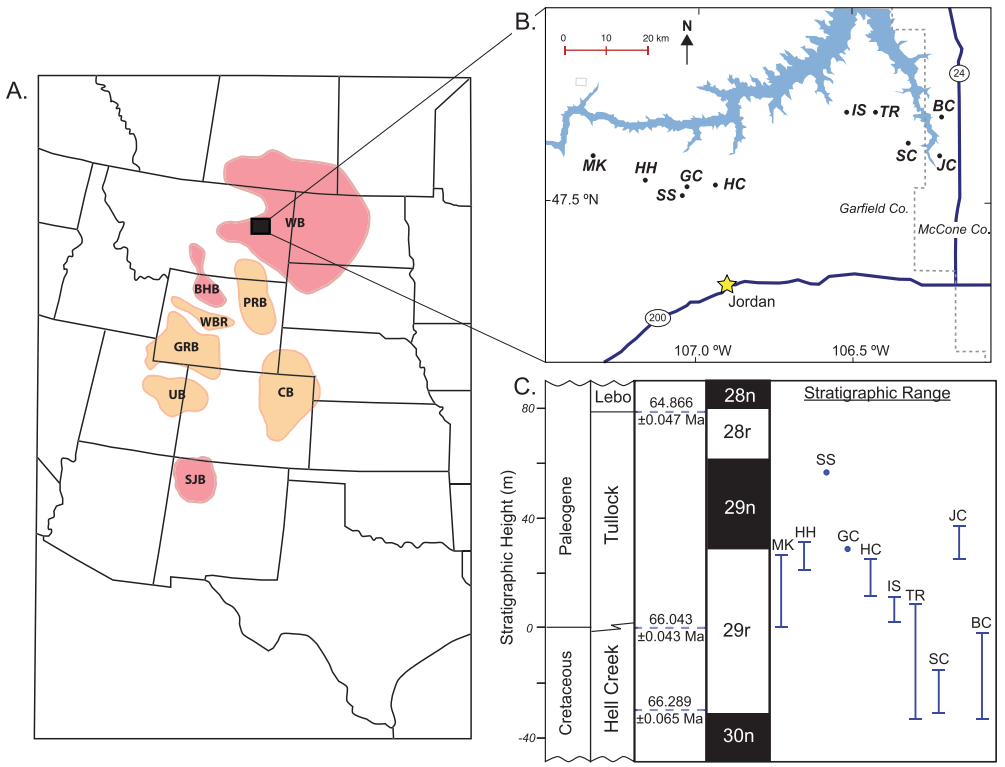

Figure 1. (a) Major foreland basin systems of the western continental United States that contain Upper Cretaceous-lower Paleogene sediments (after *Force et al*. [2001]). Basins in red indicate where intermediate titanohematite has been identified. WB: Williston basin, BHB: Big Horn basin, PRB: Powder River basin, WBR: Wind River basin, GRB: Green River basin, UB: Uinta basin, DB: Denver basin, and SJB: San Juan basin. (b) Location map of study area in the Hell Creek region of northeastern Montana. Fort Peck reservoir is shown in light blue. Labeled dots indicate locations of paleomagnetic samples used in this study. MK: McKeever Ranch, HH: Hell Hollow, GC: Garbani Channel (Hill), SS: Saddle Section, HC: Hell Creek Marina road (Lerbekmo), IS: Isaac Ranch, TR: Thomas Ranch, SC: Sandy Chicken, BC: Bug Creek, and JC: Jack's Channel. (c) Stratigraphic column showing magnetic polarity (black = normal, white = reverse) and stratigraphic range of sites shown in Figure 1b. Ages picked are for the U, IrZ (Cretaceous-Paleogene boundary), and Null coal from *Sprain et al.* [2015]. Figure after *Sprain et al.* [2015].

Lindsay et al., 1981] from the San Juan basin included limited rock magnetic analyses, which identified magnetite/titanomagnetite as the primary magnetic carriers owing to median destructive fields $\leq$40 mT. Furthermore, because the remanent magnetization of the sediments was detrital, the titanohematite recorded a direction parallel to the magnetic field, effectively masking its self-reversing property. The first study dedicated to characterizing the magnetic mineralogy of San Juan basin sedimentary rocks [*Butler*, 1982] found Curie temperatures of $\sim$200°C, not $\sim$580°C as had been expected. Holding a similar belief that intermediate titanohematite is rare in the rock record, the author concluded that the primary magnetic mineral was intermediate composition titanomagnetite. It was not until *Butler and Lindsay* [1985] revisited the rock magnetic properties of these sediments that intermediate titanohematite was recognized as the dominant ferrimagnetic mineral. Examination of magnetic separates using strong field thermomagnetic curves, X-ray diffraction (XRD), and electron microprobe analysis (EPMA) allowed *Butler and Lindsay* [1985] to conclude that the dominant ferrimagnetic mineral was intermediate titanohematite based on Curie temperatures of $\sim$200°C, rhombohedral crystal structures, and high Ti:Ti+Fe ratios. Since *Butler and Lindsay* [1985], intermediate titanohematite has been identified using similar techniques in KPg age Laramide clastic deposits across central North America, including the San Juan Basin (northwest New Mexico) [*Butler and Lindsay*, 1985; *Force et al*., 2001], the Bighorn basin (south-central Montana, north-central Wyoming) [*Butler et al*., 1987; *Force et al*., 2001], and much of the Williston basin (Western and central North Dakota and Eastern Montana, USA and Southern Alberta, Saskatchewan, and Manitoba, Canada) [*Lund et al*., 2002; *Swisher et al*., 1993; *Lerbekmo*, 1999; *Force et al*., 2001] (see Figure 1). We speculate that intermediate titanohematite is present in additional KPg age Laramide deposits, but that it has been misidentified as intermediate titanomagnetite or titanomaghemite due to inadequate rock magnetic analysis [e.g., *Peppe et al*., 2009, 2011].

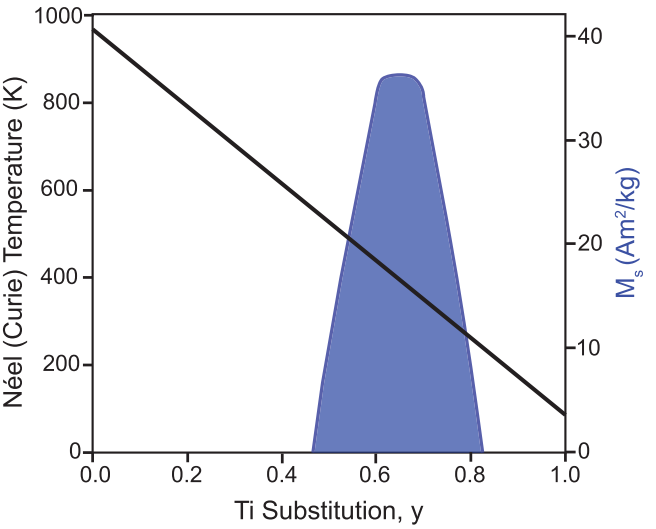

Figure 2. Effect of titanium substitution (*y*) on room-temperature saturation magnetization (Ms, blue) and Néel/Curie temperature (black) for the titanohematite solid-solution series. Blue shaded area represents region where titanohematite behaves ferrimagnetically. Figure after *Moskowitz et al*. [2015].

To facilitate the identification of intermediate titanohematite in sedimentary deposits, in this study, we characterize this mineral using low-temperature magnetometry experiments, high-temperature susceptibility measurements, and newly developed laboratory-based self-reversal experiments for KPg age sediments from the Hell Creek region, Montana. Rock magnetic characterization of intermediate composition titanohematite will help facilitate identification of this mineral in the future; moreover, by more accurately understanding its properties, it will be possible to better analyze sources of error and complexity in paleomagnetic analysis when this mineral is an important carrier of remanence. While intermediate composition titanohematite may only form in limited geologic settings, its abundance and longevity in the rock record may be more extensive than previously understood, as its self-reversing behavior can be masked by detrital remanent magnetizations (DRMs).

2. Magnetic Characteristics of Intermediate Titanohematite

Rhombohedral titanohematites ($Fe_{2-y}Ti_yO_3$) are a solid-solution series with compositions between hematite (Fe_2O_3) and ilmenite ($FeTiO_3$) end-members [*Dunlop and Özdemir*, 1997]. While the ionic substitution is exactly the same as in titanomagnetites, with Ti^{4+} substituting for Fe^{3+} and one Fe cation changing valence state from Fe^{3+} to Fe^{2+}, Ti substitution in hematite has a much more profound effect on its magnetic properties. Like hematite, titanohematite also has a corundum structure. Oxygen anions form a hexagonal-close-packed lattice, and Fe and Ti cations fill in 2/3 of the interstices, lying effectively within the basal plane. Cation distribution is disordered when titanohematite compositions are below $y \leq 0.5$, resulting in Fe^{2+} and Ti^{4+} being distributed equally in all *c* planes. This creates a magnetization very similar to hematite: antiferromagnetic with weak parasitic ferromagnetism. In this composition range the mineral behaves similarly to hematite. For compositions with $y \geq 0.5$, cation distribution is roughly ordered with Ti^{4+} and Fe^{2+} distributed in alternating cation planes, resulting in ferrimagnetism. Above compositions of $y \sim 0.8$, titanohematites are paramagnetic at room temperature but show ferrimagnetic properties at low temperatures [*Burton et al*., 2008]. The maximum saturation magnetization at room temperature occurs around $y = 0.7$, with an $M_s \sim 35$ Am^2/kg [*Moskowitz et al*., 2015] (Figure 2). Néel/Curie temperatures decrease roughly linearly with Ti substitution, with compositions above $y = 0.8$ having Curie points below room temperature [*Burton et al*., 2008] (Figure 2).

Single-phase intermediate compositions ($0.5 \leq y \leq 0.7$) can be preserved by rapid chilling of calc-alkaline intermediate to silicic lavas and pyroclastics [*Dunlop and Özdemir*, 1997]. It is within these compositions that a self-reversed thermoremanent magnetization can be acquired [*Uyeda*, 1958; *Heller et al*., 1986; *Hoffman*, 1992], although a more recent compilation of data suggests that self-reversal can occur between $0.45 \leq y \leq 0.75$ [*Fabian et al*., 2011]. In a majority of models for self-reversal in the hematite-ilmenite solid-solution series, reverse thermoremanent magnetization (RTRM) occurs due to an ordered ferrimagnetic phase being magnetized antiparallel to a magnetizing field as result of interactions with an Fe rich, more disordered phase, i.e., a weakly ferromagnetic phase or intermediate *x* phase, however the exact cause of the self-reversing process remains enigmatic (for more details see: *Nagata and Uyeda* [1959], *Nagata* [1961], *Uyeda* [1957, 1958], *Ishikawa* [1962], *Ishikawa and Syono* [1962, 1963], *Hoffman* [1975], *Kennedy and Osborne* [1987], *Nord and Lawson* [1989], *Haag et al*. [1990a,b], *Hoffmann and Fehr* [1996], *Bina et al*. [1999], *Ozima and Funaki* [2001], *Fabian et al*. [2011], and *Robinson et al*. [2012a,b]). Studies have shown that this self-

reversal is not suppressed even in fields of 2 T, suggesting that the self-reversal is caused by exchange coupling as only this mechanism can resist such high fields [*Dunlop and Özdemir*, 1997]. The primary control on self-reversal in titanohematite appears to be the coexistence of two phases in the same crystal and their exchange interactions, rather than simple interactions between repeated, highly geometric microstructures. Note that this differs from the situation in partially oxidized titanomagnetites, in which self-reversed remanence components can be produced by magnetostatic interactions, which are stronger due to the higher magnetization intensities in those minerals [*Krása et al*., 2005]. Néel/Curie temperatures within the self-reversing composition range vary from 300°C to room temperature, with coercivities ranging ~30 mT and below [*Nagata and Akimoto*, 1956; *Nagata*, 1961; *Fabian et al*., 2011] (Figure 2). It has also been observed that magnetization increases almost linearly to liquid nitrogen temperatures [*Ishikawa and Akimoto*, 1957].

While RTRM can occur over compositional ranges of $0.45 \leq y \leq 0.75$, intermediate compositions alone will not guarantee self-reversal. The development of a RTRM is strongly dependent upon thermal history and grain size [*Haag et al*., 1993; *Ozima et al*., 2003; *Ishikawa*, 1962; *Ishikawa and Syono*, 1963; *Lagroix et al*., 2004]. Samples that are entirely ordered or disordered will not show the self-reversing behavior [*Ozima et al*., 2003]. This degree of order in titanohematite is dependent upon thermal history. It has been shown that samples that have been quenched from above the ordering temperature and then annealed below the ordering temperature for short periods of time acquire a RTRM that is much stronger than for samples that were strongly annealed [*Ishikawa*, 1962; *Ishikawa and Syono*, 1962, 1963; *Fabian et al*., 2011]. This behavior has been suggested to be due to the growth of ordered domains and the decrease of antiphase boundaries during annealing [*Fabian et al*., 2011]. If the reverse ferrimagnetic phase forms domains, then it will lose its RTRM. When ordered phases are multidomain (MD), the domain boundaries acquire a reversed magnetization, but the interior of the domains respond to the applied field and acquire a magnetization parallel to the applied field and a normal TRM is recorded [*Dunlop and Özdemir*, 1997].

3. Regional Geology

The Hell Creek region of Montana holds one of the best terrestrial records of biotic and abiotic changes leading up to and across the Cretaceous-Paleogene boundary (KPB) and mass extinction. It is located within the Williston sedimentary basin in NE Montana (Figures 1a and 1b), which has been an active area of deposition since the Ordovician. Throughout the Late Cretaceous, the Hell Creek region (and much of the western interior) was covered by a shallow epicontinental sea (Western Interior Seaway) that bisected North America, extending at times from the Gulf of Mexico to the Arctic Ocean. Orogenic pulses loosely ascribed to the Laramide orogeny, coupled with rapid eustatic regression in the Late Maastrichtian resulted in major regression of the seaway, marking its last appearance in the Hell Creek region [*Gill and Cobban*, 1973]. The seaway persisted in the northern Western Interior through the end Cretaceous and had a short transgressive period in the early Paleocene, marked by marine formations deposited from the Cannonball Sea in North and South Dakota [*Boyd and Lillegraven*, 2011]. The Hell Creek Formation (mostly Cretaceous) and Tullock Member of the Fort Union Formation (mostly Paleogene) in the Hell Creek region comprise fluvial deposits that formed as a prograding clastic wedge following the eastward advancement of the Sheridan Delta due to the rapid retreat of the Western Interior seaway [*Fastovsky*, 1987]. The Hell Creek Fm./Tullock Mb. formational boundary is roughly coincident with the KPB. These formations are correlative with other fluvial deposits within the Williston basin including the Hell Creek Formation and Ludlow Member of the Fort Union Formation in North Dakota and South Dakota and the Frenchman and Ravenscrag Formations in Canada [*Hartman*, 2002; *Hartman et al*., 2014]. Rock types included in these deposits include siltstone, mudstone, fine sandstone, and lignite, representative of flood plain deposition, and coarser sandstones, representative of channel deposition.

Thin, distal volcanic tephra layers are preserved within lignite deposits in the Hell Creek region. These layers contain minerals amenable to both high-precision $^{40}Ar/^{39}Ar$ dating, and U/Pb dating [*Renne et al*., 2013; *Sprain et al*., 2015], and have yielded precision as good as 40 ka [*Renne et al*., 2013; *Sprain et al*., 2015]. $^{40}Ar/^{39}Ar$ and U/Pb ages of tephra layers, combined with magnetostratigraphy, form the geochronologic framework for a variety of studies on biotic and abiotic terrestrial processes associated with the mass extinctions. Thus, a well-grounded understanding of the magnetic minerals recording the magnetostratigraphy in this region is essential.

Table 1. Magnetic Properties of Laramide Sediments[a]

Location	Curie T Range (°C)	AF Demag Range (mT)	Tub (°C)	Age	Chrons	Mineral ID	IRM Acquisition	XRD	EPMA	Paper
BHB, WY	180–250,[b] 580[b]	30	N/A	Late Pal.-Eoc.	C27r-C25r	M/TM, TH[b]	<300 mT	Y[b]	Y[b]	*Butler et al.* [1981][b]
SJB, NM	180–300[b]	20–60	N/A	Late Cret.-Pal.	C31n-C25r	M/TM, TH[b]	N/A	Y[b]	Y[b]	*Lindsay et al.* [1981][b]
BHB, MT	150–250	10–40	<300	Late Pal.	C27r-C26r	TH	200–300 mT	Y[b]	Y[b]	*Butler et al.* [1987][b]
WB, MT	160–200	20–80	<300	Late Cret.-early Pal.	C30n-C28n	TH	<300 mT	Y[b]	Y[b]	*Swisher et al.* [1993][b]
WB, MT	N/A	2.5–50	N/A	Late Cret.-early Pal.	C30r?-C28n	N/A	N/A	N	N	*LeCain et al.* [2014]
WB, ND	<225	10–50	100–300	Late Cret.-early Pal.	C30n-C29n	TH	N/A	Y	Y	*Lund et al.* [2002]
WB, MT	200[b]	20–80	N/A	Late Cret.-early Pal.	C30n-C29n	M/TM, TH[b]	<300 mT	Y[b]	Y[b]	*Archibald et al.* [1982][b]
BHB, WY	~200, 580	N/A	N/A	Late Cret.-early Pal.	N/A	TH, M	N/A	Y	Y	*Force et al.* [2001]
WB, MT	~200	N/A	N/A	Late Cret.-early Pal.	N/A	TH	N/A	Y	Y	*Force et al.* [2001]
WB, Canada	N/A	10–30	100	Late Cret.-early Pal.	C33n-C26r	TM, M, TH	N/A	N/A	N/A	*Lerbekmo* [1999]
WB, Canada	N/A	10–30	N/A	Late Cret.-early Pal.	C33n-C29r	TM, M	N/A	N/A	N/A	*Lerbekmo and Coulter* [1985]
WB, ND	450–580, some 180–200	N/A	250–400	Late Cret.-early Pal.	C29n-C27r	TMH	>100 mT	N/A	EDS	*Peppe et al.* [2009]
PRB, MT	N/A	N/A	250–400	Early Pal.	C29n-C26r	TMH	N/A	N/A	N/A	*Peppe et al.* [2011]

[a]Magnetic properties of Upper Cretaceous-lower Paleogene sediments from Laramide-Style basins within the Western U.S. Location indicates major foreland basin and U.S. State, unless conducted outside the U.S. BHB: Big Horn basin, SJB: San Juan basin, WB: Williston basin, and PRB: Powder River basin. AF demag range shows either the alternating field (AF) at which the characteristic remanent magnetization (ChRM) could be constrained, or the range of AFs over which the ChRM was removed. T_{UB} is the unblocking temperature determined from thermal demagnetization experiments. Mineral ID is the magnetic mineral attributed with carrying primary remanence. M: Magnetite, TM: Titanomagnetite, TH: Intermediate titanohematite, TMH: Titanomaghemite. IRM acquisition indicates the field at which saturation was reached.
[b]Reanalyzed in *Force et al.* [2001].

Provenance studies of the Hell Creek Formation and Tullock Member in the Hell Creek region are limited. However, analysis of paleocurrent directions in the early Paleocene suggest that sediment was transported to the east from central Montana and northeast, across the Powder River Basin in southern Montana, into the Williston basin [*Cherven and Jacob*, 1985] (Figure 1). These trends are compatible with sandstone compositions indicating a dominantly volcanic-metamorphic provenance for Late Cretaceous sediments, associated with Laramide (in a broad sense) magmatic arc volcanism to the west (likely western Montana or eastern Idaho), and mixed volcanic and sedimentary detritus for early Paleocene deposition, indicative of the propagation of retroarc thrust belts and uplift of supracrustal sedimentary rocks like the Bighorn Mountains and Black Hills to the southwest [*Cherven and Jacob*, 1985]. A suggested source for the volcanic detritus is the Elkhorn Mountains [*Cherven and Jacob*, 1985; *Gill and Cobban*, 1973; *Force et al.*, 2001] in southwestern Montana, which consist of the eroded remnant of a volcanic plateau that comprises calc-alkaline silicic to intermediate lavas and tuffs. This volcanic environment is amenable to the formation of intermediate titanohematite, however, RTRMs have not been documented for the Elkhorn rocks [*Diehl*, 1991]. Based on stratigraphic and paleontological data, the Elkhorn volcanics have been dated to the early Campanian, ~80 Ma. Due to the abundance of Laramide volcanic centers in the Late Cretaceous, it is equally possible that another volcanic center, such as the Idaho Batholith, is the sediment source for the Hell Creek Formation and Tullock Member.

Magnetostratigraphic analysis is actively used in the Hell Creek as a means to correlate paleontological records across the region [*Archibald et al.*, 1982; *Swisher et al.*, 1993; *LeCain et al.*, 2014]. Of the multiple magnetostratigraphic studies, only one study completed rock magnetic analysis [*Swisher et al.*, 1993] (data published in *Force et al.* [2001]). Magnetic mineralogy was characterized using strong-field thermomagnetic analysis, X-ray diffraction (XRD), electron microprobe analysis (EPMA), and room temperature IRM acquisition [*Swisher et al.*, 1993; *Force et al.*, 2001]. Curie temperatures were found to be between 160° and 200°, with X-ray diffraction and EPMA results indicating an intermediate-composition titanohematite as the dominant ferromagnetic mineral [*Swisher et al.*, 1993]. In all Hell Creek paleomagnetic studies, coercivity spectra reveal that the characteristic remanent direction is constrained between 20 and 80 mT [*Archibald et al.*, 1982; *Swisher et al.*, 1993; *LeCain et al.*, 2014] (Table 1). These results are similar to those observed for other KPg Laramide continental deposits in the San Juan Basin, NM, Big Horn Basin, WY and MT, Powder River Basin, WY and MT, and other parts of the Williston Basin (southeastern MT, southern Canada, and eastern and central North Dakota) [*Butler et al.*, 1981; *Lindsay et al.*, 1981; *Butler et al.*, 1987; *Peppe et al.*, 2009, 2011; *Lerbekmo and Coulter*, 1984, 1985; *Lerbekmo*, 1999; *Lund et al.*, 2002]. No further rock magnetic analyses have been conducted on rocks from the Hell Creek region since *Swisher et al.* [1993]. The goal of our study is to update the magnetic characterization of rocks from the Hell Creek region using modern equipment

and techniques, to test previous results, and to understand the degree to which intermediate titanohematite may influence the fidelity of magnetostratigraphic records in Laramide basins throughout the central United States.

4. Methods

4.1. Sampling

Oriented block samples for paleomagnetic analysis were collected from siltstones, mudstones, and fine-grained sandstones across both the Hell Creek Fm. and Tullock Mb. of the Fort Union Fm. (Figures 1b and 1c). For each sampling horizon, three block samples were collected. Two to three 16 cm^3 specimen cubes were cut from each block sample. When an oriented sample was not needed, chips taken from original block samples were used. Oriented cubes were cut and subjected to stepwise thermal and AF demagnetization and remanence measurements at the Berkeley Geochronology Center. Directional results will be published in a future contribution. To obtain magnetic extracts, rock chips were crushed using a rubber mallet and ground to an appropriate size using a mortar and pestle. For samples with abundant magnetic material, extracts were obtained using a Nd-hand magnet with a plastic sleeve. Extracts from samples with sparse magnetic material were collected using either the pump extraction or flask extraction method described in *Strehlau et al.* [2014]. All extracts were obtained at the Institute for Rock Magnetism at the University of Minnesota.

4.2. Rock Magnetic Measurements

Rock magnetic experiments were conducted at the Institute for Rock Magnetism at the University of Minnesota. High-temperature, low-field susceptibility experiments were conducted on seven whole-rock samples and seven magnetic separates using a Geofyzika KLY-2 KappaBridge AC susceptibility meter with an AC field of 300 Am^{-1} and a frequency of 920 Hz. Heating of whole-rock samples was two cycled, starting at room temperature and going up to 300°C, cooling to room temperature, and then heating from room temperature to 600°C, and cooling back to room temperature. Of the seven extracts, four underwent multicycled heating with peak temperatures every 100°C, ending at 400°C. One additional extract was heated similarly up to 600°C. The two remaining magnetic extracts were heated without cycling from room temperature up to 600°C and then back to room temperature. Measurements were collected on warming and cooling. Of the 14 high-temperature susceptibility experiments, two were measured in argon. The other 12 samples were run in air. Néel/Curie temperatures were determined by taking the first derivative of the measured data [*Fabian et al.*, 2013].

Low-temperature experiments were run on a Quantum Design Magnetic Properties Measurement System (MPMS-5S). Thirty-five specimens were run on the MPMS, 11 specimens underwent the FC-ZFC-LTSIRM-RTSIRM protocol, and 24 underwent the more abbreviated sweep-cool-warm (or warm-cool) protocol (see *Bilardello and Jackson* [2013] for more details). The FC-ZFC-LTSIRM-RTSIRM protocol involves first applying a sustained DC field of 2.5 T on a sample as it cools from room temperature to 20 K (field cooling, FC). The field is then turned off and the remanence upon warming to 300 K is measured. The sample is then cooled back to 20 K (zero-field cooling, ZFC) and a 2.5 T low-temperature saturation isothermal remanent magnetization (LTSIRM) is imparted. Remanence is again measured upon warming to room temperature (and is referred to as the ZFC remanence). Once at room temperature, a 2.5 T SIRM (RTSIRM) is applied and remanence is measured upon cooling to 20 K, and again during warming back to room temperature. Under the sweep-cool-warm protocol, the sample is first given a 2.5 T RTSIRM and then remanence is measured as the sample is cooled to 20 K. At 20 K, a 2.5 T LTSIRM is imparted and the remanence is measured upon warming to 300 K (also known as ZFC). Under the sweep-warm-cool protocol, the RTSIRM and ZFC are switched. Measurements were taken for both protocols every 5 K.

Major hysteresis loops and backfield curves for 35 specimens were measured at room temperature using a MicroMag Princeton Measurements vibrating sample magnetometer (VSM) with a nominal sensitivity of 5×10^{-9} Am^2. First-order reversal curves (FORCs) were obtained for four specimens including two magnetic extracts on both the VSM and the MicroMag Princeton Measurements Alternating Gradient Magnetometer with a sensitivity of 1×10^{-11} Am^2. FORC data were processed using the FORCinel software of *Harrison and Feinberg* [2008].

To further understand the mineralogy and range of coercivities present in our samples, a triaxial-IRM Lowrie test was conducted on 18 oriented cubes [*Lowrie*, 1990]. Three orthogonal IRM's were sequentially imparted on the specimens in fields of 1 T, 300 mT, and 100 mT using an ASC pulse magnetizer. Samples were then stepwise thermally demagnetized up to 550°C in an ASC Model TD-48SC Thermal Demagnetizer with a TRM field coil. Samples were measured on a 2G Superconducting Magnetometer with nominal sensitivity of 2×10^{-11} Am^2 inside a magnetically shielded room with background fields $\leq$200 nT.

In order to further evaluate the presence of intermediate titanohematite in our samples we developed a self-reversal test. First, the NRM of the sample was measured. Next, we imparted a partial TRM using a 100 μT field with a declination and inclination of 0° and 0°, at a peak temperature of 300°C, for a soak time of 30 min in a ASC Model TD-48SC Thermal Demagnetizer with a TRM field coil for 13 oriented cubic specimens. The 300°C peak temperature was chosen to ensure that any self-reversing titanohematite acquired a RTRM, but also to avoid any dramatic mineralogic alteration to the sediment samples. Specimens were then measured and subjected to stepwise alternating field (AF) demagnetization up to fields between 150 and 170 mT. Measurements and AF demagnetization were conducted using the U-Channel Superconducting Rock Magnetometer (2G Enterprises, Inc. 755, DC-4K Liquid Helium Free SQUID) with inline ARM and offline IRM capabilities. Specimens whose magnetic remanence is dominated by self-reversing titanohematite should show a TRM that is oriented antiparallel to the applied field direction (declination 180°, inclination 0°). Specimens that contain a mixture of magnetic minerals that record a remanence parallel to an applied field (e.g., magnetite, titanomagnetite, goethite, and nonself-reversing titanohematite) and nearly antiparallel to an applied field (self-reversing titanohematite) should show a demagnetization path that falls along a great circle in equal area projection between 0° and 180°. Samples with negligible self-reversing minerals should show no great circle behavior and should instead show circular clustering parallel to the applied field direction. Depending on the relative rates of removal of the parallel and antiparallel components, the total TRM intensity may also show diagnostic patterns of variation during stepwise demagnetization.

4.3. Non-magnetic Analysis

To further constrain mineralogy, X-ray diffraction (XRD) and electron microprobe analysis (EPMA) were conducted on magnetic extracts at the University of California, Berkeley. XRD patterns were collected for six samples using a PANalytical X'Pert Pro diffractometer equipped with a Co-K_α source. Extracts were mixed with acetone and placed on silicon zero background plates, which were then mounted onto the XRD sample stage for pattern acquisition. Collection times were optimized for each sample and ranged from 25 min to 3 h. The X'Pert HighScore PANalytical software was used for analysis accessing the PDF-2 2003 release database.

Sample compositions for three magnetic extracts were measured by electron probe microanalysis (EPMA) with a Cameca SX-51 in the Department of Earth and Planetary Science at the University of California, Berkeley. Analyses were conducted with 15 keV accelerating voltage, 20 nA beam current, and 1 μm beam diameter. Elements were acquired using analyzing crystals LIF for Fe kα, Mn kα, PET for Ti kα, Ca kα, TAP for Mg kα, Al kα, and NICRBN for O kα. On and off peak counting times were 20 s for all elements, except O kα for which the on and off peak count time was 40 s.

To inspect the optical properties of our magnetic minerals further, scanning electron microscope (SEM) images using backscattered electrons (BSE) were collected for magnetic extracts. SEM analysis was carried out on a Zeiss EVO Variable Vacuum Instrument −10 SEM at the University of California, Berkeley. Qualitative chemical analysis was performed with an energy-dispersive X-ray detector (EDS) and elemental analysis was performed on the EDAX system with a silicon drift detector and thin windows, which detect down to Boron.

5. Results

The determination of Néel/Curie temperatures from high-temperature susceptibility, χ(T), measurements was unsuccessful for whole-rock specimens because response was not reversible between heating and cooling cycles. The irreversibility was likely caused by alteration of Fe-bearing clay minerals to form magnetite during heating, suggested by a susceptibility increase upon cooling. Alteration appears minimally at temperatures below 350°C, and occurs primarily at temperatures between 350°C and 600°C. High-

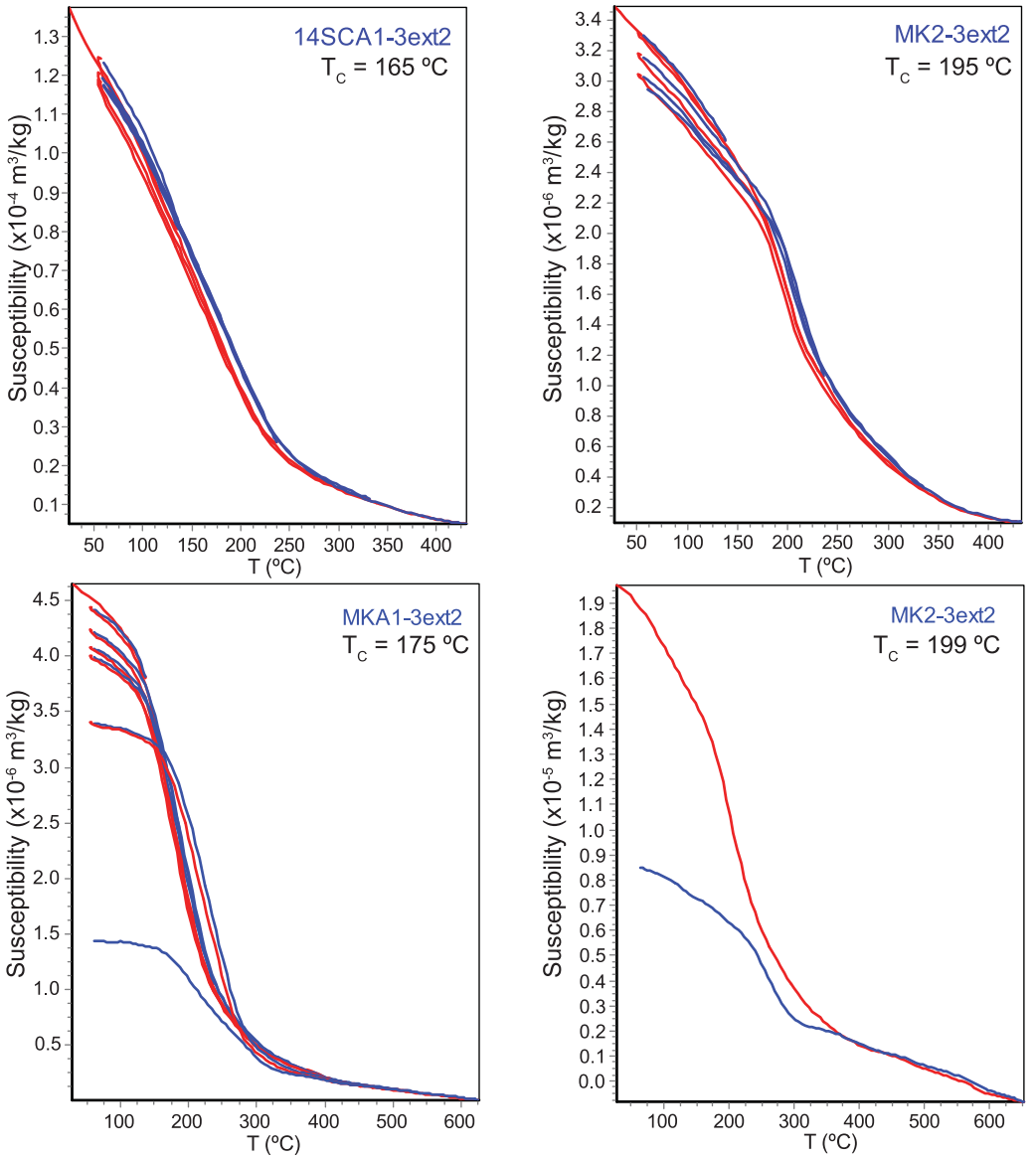

Figure 3. High-temperature heating (red) and cooling curves (blue) of bulk magnetic susceptibility, in air and argon (14SCA1-3ext2 only), for representative magnetic extracts. Néel/Curie temperatures (Tc) are indicated in the upper right of each plot.

temperature susceptibility experiments on magnetic extracts were much more successful. For all specimens, temperature curves were reversible below 400°C and show Néel/Curie temperatures ranging from ~100°C to 200°C (Figure 3). These data are consistent with the estimates from *Swisher et al*. [1993] for rocks from the Hell Creek region, and is in the range of expected Néel/Curie temperatures for intermediate composition titanohematite. Titanohematite compositions were determined from Néel/Curie temperatures using the calibration of *Moskowitz et al*. [2015] and range from $y = 0.53–0.63$ (Figure 3). For two specimens, a second Néel/Curie temperature is found around 580°C (Figure 3). While this temperature is indicative of the presence of magnetite, it is difficult to say from these data alone whether magnetite is a primary mineral found within the sample, or if it was a laboratory-induced by-product of alteration upon heating, potentially from clay minerals in impure magnetic extracts. Fortunately, the low-temperature magnetometry data help address this ambiguity. Extracts that were heated beyond 400°C show irreversibility between heating and cooling curves (Figure 3). Unlike whole-rock specimens, cooling curves for extracts show a drop in susceptibility suggesting that irreversibility may be caused by oxidation of a magnetic mineral, potentially titanomaghemite.

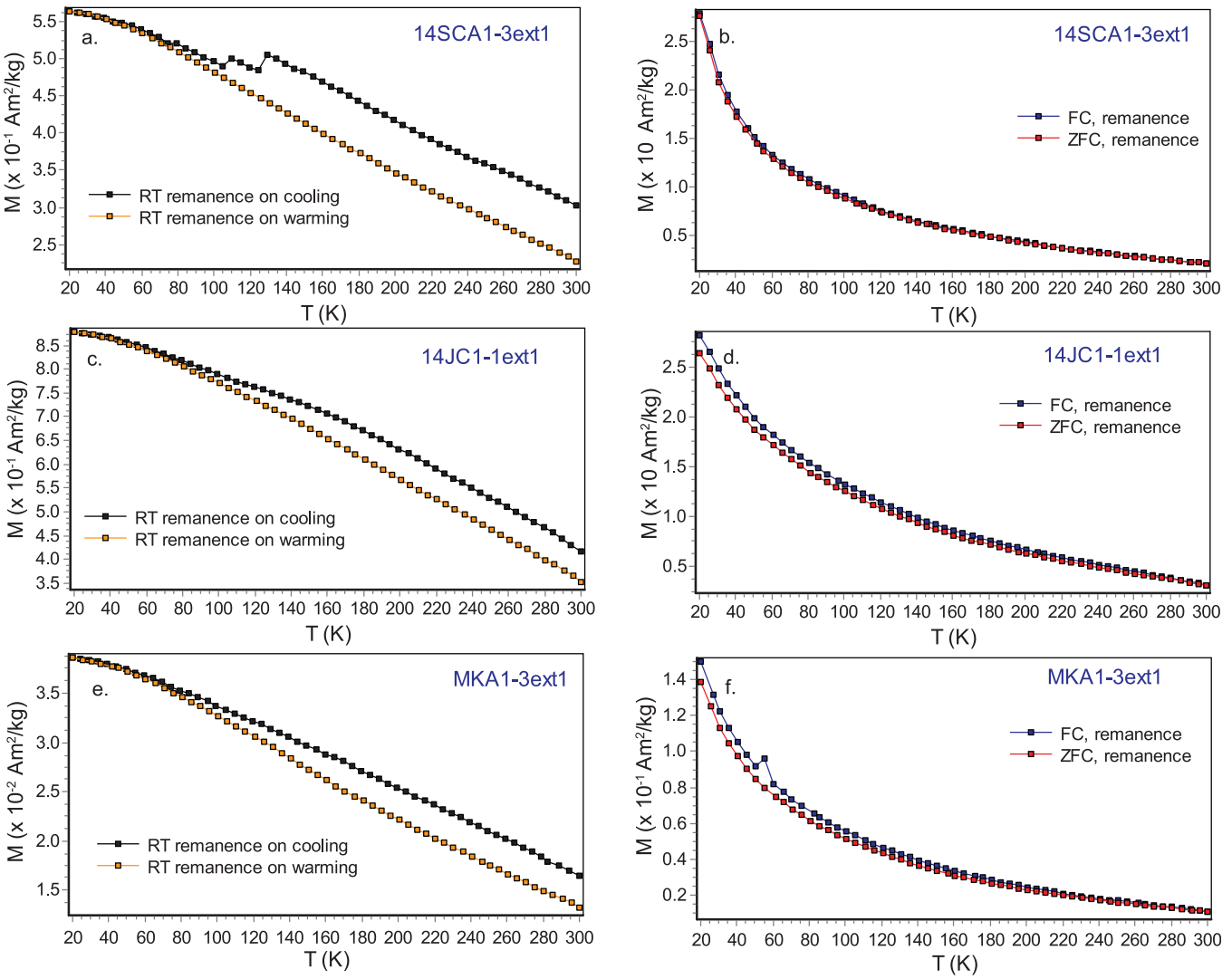

Figure 4. Low-temperature magnetization curves on magnetic extracts for representative samples. (left) Measurements of magnetization (M) during cooling (black) and warming (orange) following the application of a saturation isothermal remanent magnetization (SIRM) applied at room temperature (RT). (right) Measurements of magnetization during warming following a sustained direct current field of 2.5 T during cooling (field-cooled, FC: blue), and measurements of magnetization during warming following a SIRM imparted at low temperature (zero field-cooled, ZFC: red). Note: spikes in magnetization in Figures 4a and 4f are measurement artifacts.

The low-temperature magnetometry experiments showed signs of magnetite and/or titanomagnetite in 90% of the samples. The Verwey transition occurs at ~120 K in stoichiometric magnetite and is a first-order phase transition from cubic to monoclinic crystal symmetry. The Verwey transition does not occur in Ti-substituted forms of magnetite, but a similar low-temperature behavior is observed associated with a change in sign of the mineral's magnetocrystalline anisotropy constant at a temperature that depends on Ti content [*Moskowitz et al.*, 1998; *Church et al.*, 2011]. When magnetite and titanomagnetite grains become partially oxidized ("maghemitization") these transitions occur over broader temperature ranges and eventually become completely smeared out, making it difficult to determine if a sample contains pure magnetite or titanomagnetite. This latter behavior was expressed by 90% of the samples in this study (Figures 4 and 5).

For all specimens (whole-rock and magnetic extract), RTSIRM curves show a near twofold increase in remanence toward lower temperatures (Figure 4). Results from the FC-ZFC-RTSIRM-LTSIRM protocol also show a significant remanence gain on RTSIRM cooling (Figure 4). While at first glance, the twofold increase in remanence on RTSIRM cooling appears diagnostic of goethite [e.g., *Lowrie and Heller*, 1982; *Dekkers*, 1989; *France and Oldfield*, 2000], this feature is also present for magnetic extracts (Figure 5), which likely do not contain

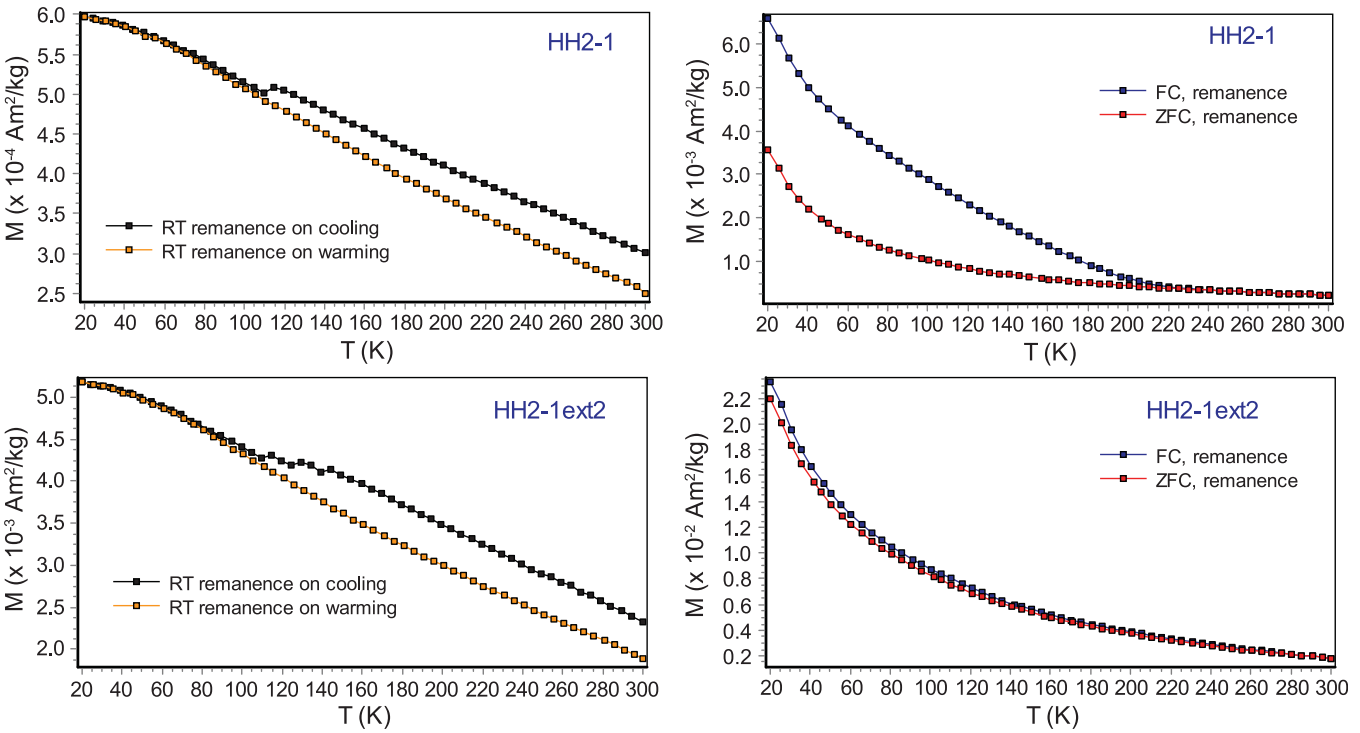

Figure 5. Low-temperature magnetization curves for a whole-rock sample (HH2-1) and a magnetic extract (HH2-1ext2) from the same specimen. Notice that the large spread between the field-cooled (FC) and zero field-cooled (ZFC) curves for the whole-rock sample is not present for the magnetic extract but the RTSIRM curves remain similar.

goethite, because it is difficult to extract using common magnetic separation techniques. Proof of the absence of goethite in magnetic extracts exists in FC-ZFC measurements as one of goethite's diagnostic features, a wide spread between FC and ZFC remanences, is absent for all specimens except one (Figure 5). A likely explanation for this observed trend is that the increased intensity toward lower temperatures is due to the presence of intermediate-composition titanohematite, not goethite, as it also has a low-ordering temperature (~200°C), and therefore spontaneous magnetization increases strongly on cooling.

Hysteresis data are consistent with the presence of a low-coercivity ferromagnetic mineral, indicated by low (<10 mT) bulk coercivities, and backfield curve saturation well below 1 T; some samples however have a higher-coercivity tail which we suggest is due to the presence of goethite and/or hematite. Paramagnetic minerals make up a large percentage of the magnetic signal consistent with the abundance of clays in our samples. Plotting hysteresis data on a Day plot (Figure 6) with the mixing curves from *Dunlop* [2002] show that the dominant mineralogy of our samples is not pure magnetite. While samples appear to plot in a roughly congruent pattern, they show higher Bcr/Bc ratios than magnetite and fall to the right of the Dunlop mixing lines. Looking at the data on a squareness-coercivity plot (Mr/Ms versus Bc: Figure 7), we see that our data plot in a linear trend, suggesting that our samples have similar mineralogies but varying grain sizes. Plotting the trends for low Ti-magnetite and TM60 [*Wang and Van der Voo*, 2004], we see that our data plot between the trends, suggesting that our samples are likely oxidized.

FORC data were collected to further assess the distribution of coercivities in both whole-rock samples and magnetic separates. FORC diagrams for both sample types show a strong coercivity peak around 5 mT with strong interaction fields (Hu) extending in both the positive and negative direction to ±20 mT along the Hu axis (Figure 8). This peak is most likely representative of the pseudo single-domain grains within our samples and is consistent with the measured bulk coercivities measured from the major hysteresis loops. In addition to the low coercivity peak, considerably higher-coercivity grains extend out along the Hu = 0 axis to as far as 70 mT, indicating populations of stable-single-domain grains. These high-coercivity grains are more apparent in the whole-rock samples, suggesting that the magnetic separation techniques used in this study are biased toward the collection of larger sized particles (e.g., PSD and MD), as SD size grains may adhere to clay particles removed during the extraction.

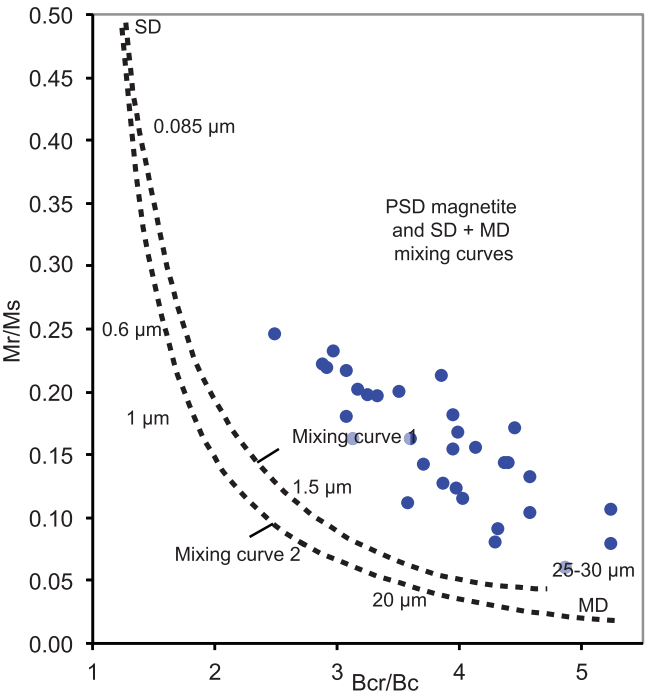

Figure 6. Day plot of hysteresis ratios (Mr/Ms versus Bcr/Bc) for all measured whole-rock specimens [*Day et al.*, 1977]. Dotted curves indicate theoretical mixing curves of single-domain (SD) and multidomain (MD) magnetite grains after *Dunlop* [2002]. All data fall to the right of the mixing curves, suggesting that magnetite does not control the hysteresis properties of our samples.

Thermal demagnetization of isothermal remanent magnetizations (IRM) applied along the X, *Y*, and *Z* axes of representative samples shows that for the majority of samples the IRM is held by grains whose coercivities fall between 0 and 300 mT, with a majority of remanence held between 0 and 100 mT (Figure 9). Very little remanence is held between 300 mT and 1 T, however, it is evident that the small amount of remanence held in this component is removed around 300°C, consistent with unblocking temperatures for intermediate titanohematite. Remanence held between 0 and 100 mT, and 100 and 300 mT shows an almost continuous drop in remanence between 100 and 300°C and a sharper drop between 300 and 400°C, consistent with the presence of both intermediate titanohematite (with Tc between 100 and 200°C) and titanomagnetite(-maghemite) (most evident within the higher 300–400°C range). Remaining remanence after 400°C is likely held by magnetite or titanomagnetite(maghemite), observed in both high-T susceptibility experiments (although it might be due to alteration) and low-temperature experiments. For a few samples (e.g., HHA1-3B in Figure 9), a large drop in remanence for all coercivities occurs around 100°C, consistent with the presence of intermediate titanohematite.

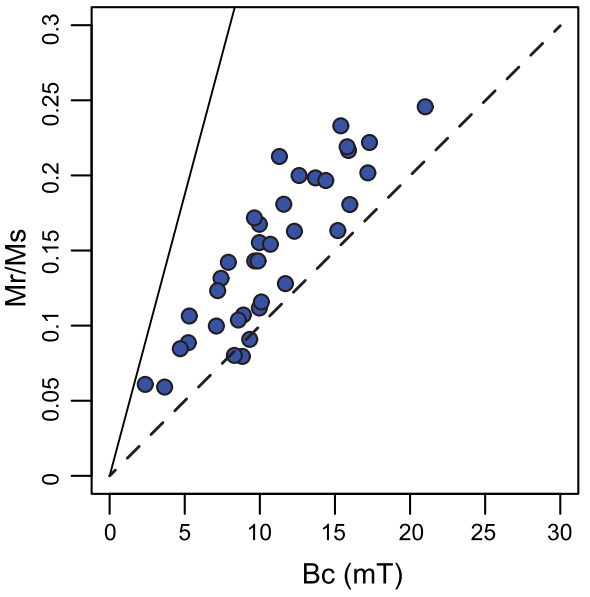

Figure 7. Squareness plot (Mr/Ms versus Bc) for all measured whole-rock specimens. Solid and dotted lines show trends for TM60 and low-Ti magnetite after *Wang and Van der Voo* [2004]. Data form a linear trend falling between the two lines, indicating that our samples share similar mineralogies, which are not solely magnetite or titanomagnetite.

Results from the self-reversal test show that all whole-rock samples have a component that acquires thermoremanent magnetization parallel to the applied field. This component could be held by titanomagnetite or maghemite with blocking temperatures below 300°C, or by titanohematite with disordered domains that have Néel/Curie temperatures higher than the applied temperature (in which case the ordered domains would not acquire an antiparallel direction), or by goethite. Of the 13 samples run, 2 show complete reversal from the applied direction after demagnetization to AF steps between 150 and 170 mT. One such sample, MKA1-3D, is shown in Figure 10, where demagnetization data trace a clear great circle path on a stereonet, reaching an orientation nearly orthogonal to the TRM field direction after 50 mT demagnetization, and continuing to change progressively up to the maximum AF treatment of 130 mT, after which it is very nearly antiparallel to the TRM field direction. The moment of the

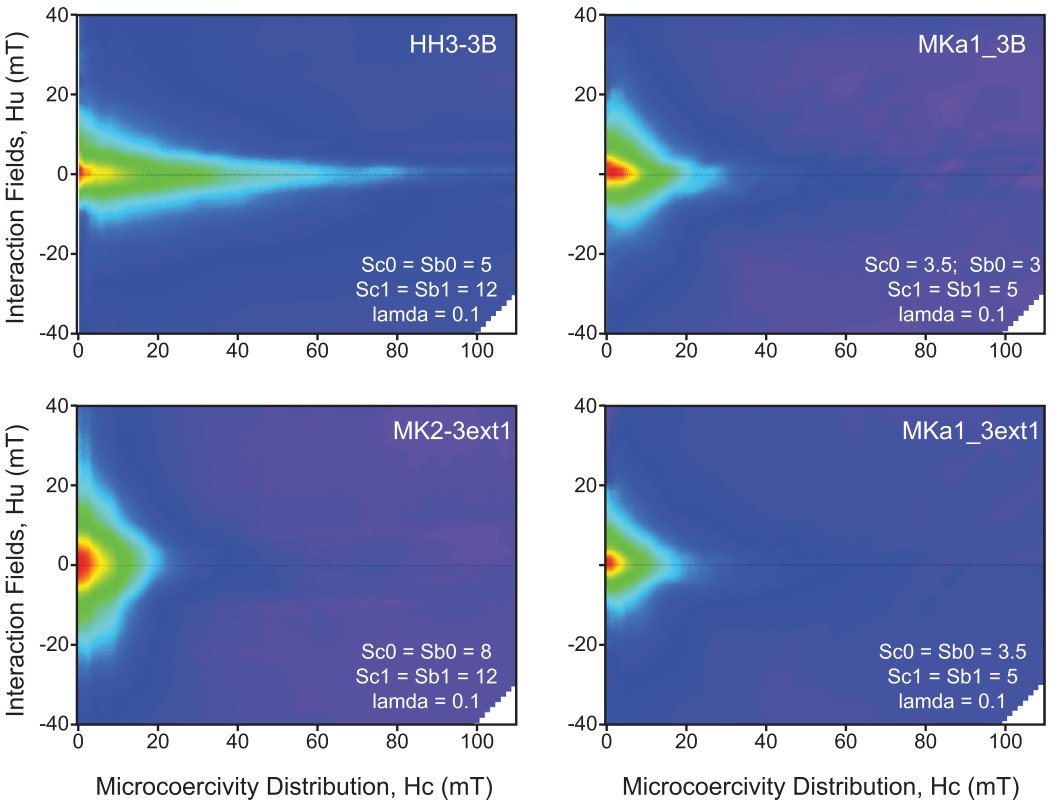

Figure 8. FORC distributions for two whole-rock samples (HH3-3B and MKa1_3B) and two magnetic extracts (MK2-3ext1 and MKa1_3ext1) from the Hell Creek region. Each specimen shows varying combinations of PSD grains and noninteracting, stable SD grains, however, SD populations are smaller in magnetic extracts. Distributions were produced using FORCinel v.2.02 [*Harrison and Feinberg*, 2008] and the VARIFORC method of *Egli* [2013]. Each FORC distribution was produced after subtracting an averaged lower branch and removing the first point artifact.

sample initially decreases strongly, reaching a minimum near 50 mT where the *x* component (parallel to the TRM field) changes sign, and then increases progressively as the field-parallel TRM is removed more rapidly than the antiparallel RTRM. This behavior is strongly suggestive of the presence of intermediate titanohematite, and is consistent with earlier studies that show self-reversing titanohematite to have slightly more elevated coercivities than magnetite and titanomagnetite [*Lawson et al.*, 1987; *Goguitchaichvili and Prévot*, 2000]. Of the remaining samples, five specimens show incomplete trends toward the antiparallel direction during demagnetization, which could be caused by a stronger overlap in coercivity between minerals holding the parallel and antiparallel components. An example of this behavior (HHA3-2D) is shown in Figure 10. The acquisition of the antiparallel direction in some of these samples suggests that the intermediate titanohematite present is SD to PSD in grain size because self-reversal is unlikely to occur in MD size intermediate titanohematite grains [*Dunlop and Özdemir*, 1997].

Four specimens showed little sign of any remanence antiparallel to the applied field direction. These specimens acquired a direction slightly offset from the applied field direction and trended toward the applied field during AF demagnetization. One specimen acquired a direction slightly offset from the applied field and did not show any change with AF demagnetization (HH1-1C in Figure 10). While it is possible that these particular samples contain intermediate titanohematite with low coercivity, which would therefore be removed first during AF demagnetization, it is more likely given the elevated coercivities observed in earlier studies, that this specimen does not contain intermediate titanohematite. Instead, the remanence of this sample is held almost entirely by minerals that acquire a thermoremanence parallel to an applied field.

XRD analysis shows that for four of the six magnetic extracts, the diffraction peaks of the Fe-Ti oxides best-align with those of an ilmenite standard, indicating that the oxides have rhombohedral crystal structures consistent with intermediate titanohematite (Figure 11). Titanomagnetite was only identified in one sample in which ilmenite is also identified. However, upon reanalysis using a longer collection time,

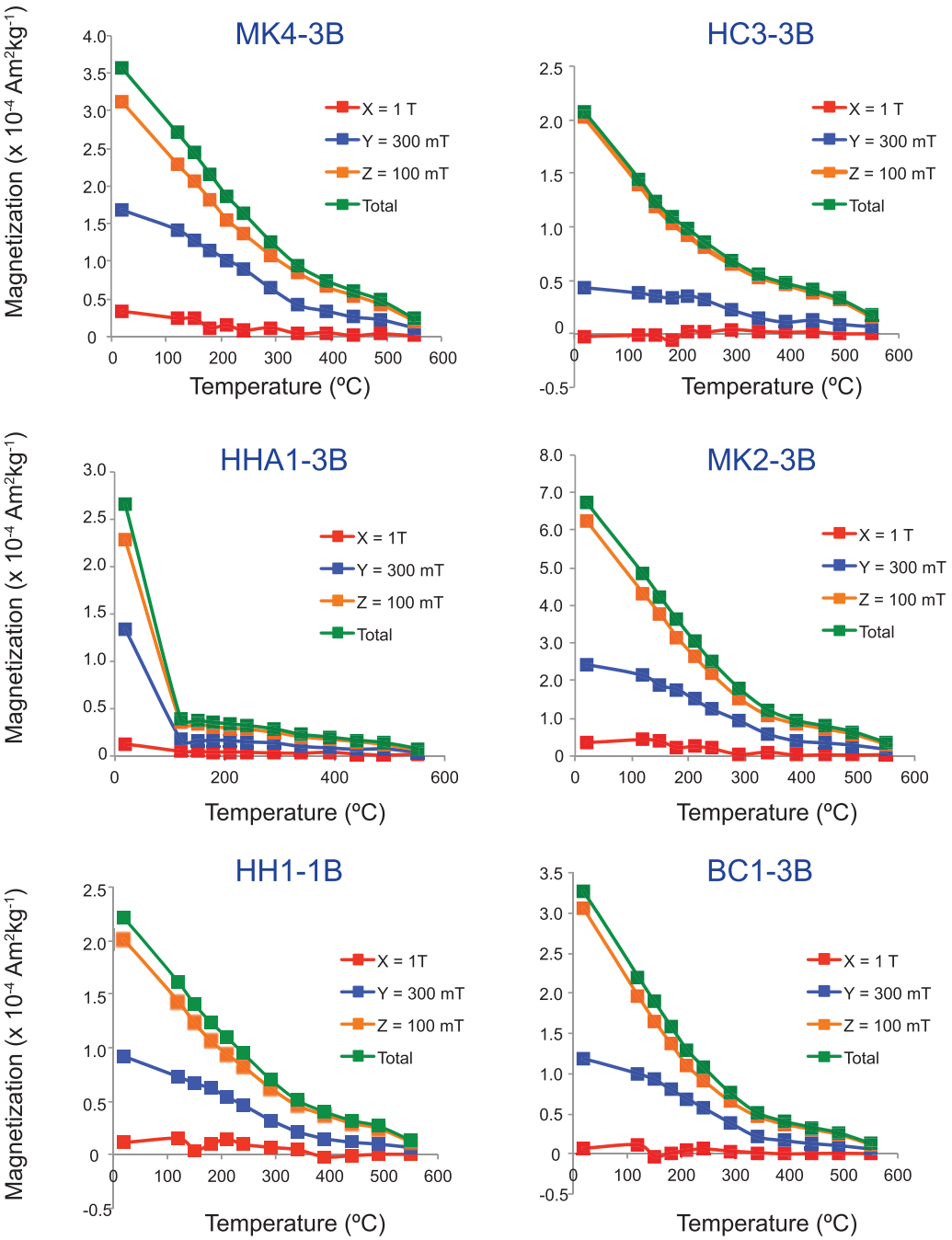

Figure 9. Thermal demagnetization of isothermal remanent magnetization (IRM) imparted along orthogonal *X*, *Y*, and *Z* axes for six selected specimens. Peak DC fields for each axis are noted. Approach follows that of *Lowrie* [1990].

titanomagnetite no longer appears as a best-match mineral. One sample did not yield good results due to the small size of the extract. Pure end-member magnetite was not identified in any of the six analyses, but this is not surprising given that the detection limit for most XRD systems is 1% by mass. The sensitivity of rock magnetic measurements is much higher by comparison.

Results from EPMA analysis were used to calculate Ti:Ti+Fe ratios for each grain, from which an average and standard deviation for each magnetic extract were calculated. Within an extract, Ti:Ti+Fe ratios are consistent, with standard deviations of no more than 6% of the average value. The calculated Ti ratios for the samples ranged from 0.245 to 0.303 and are only consistent with titanomagnetite compositions ($Fe_{3-x}Ti_xO_4$) where $x \geq 0.74$, which would correspond to Curie temperatures $\leq$70°C; this is far too low to explain the

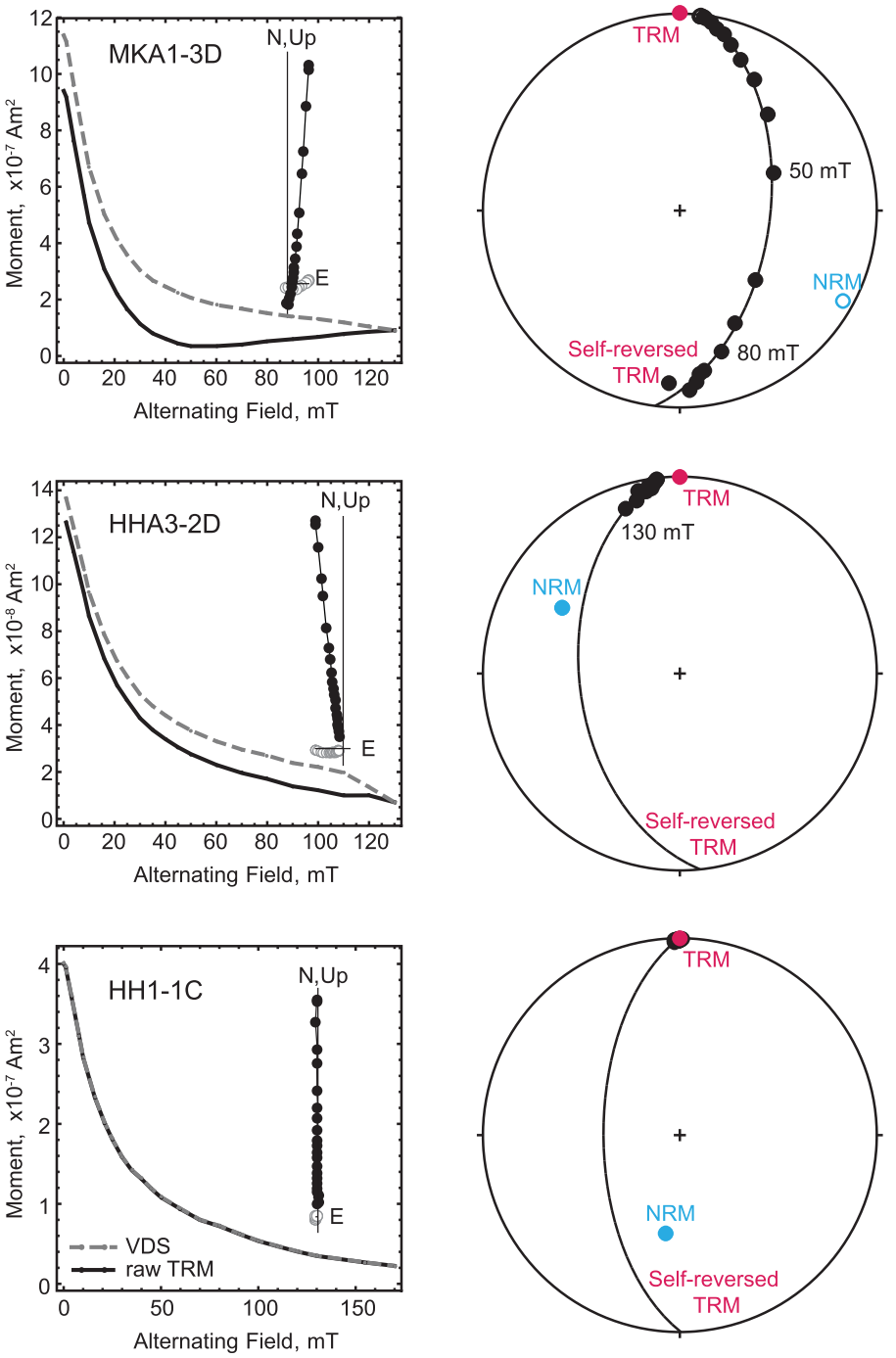

Figure 10. Demagnetization data from self-reversal tests showing three varieties of behavior. Plots on left show the intensity of the TRM during AF demagnetization, with orthogonal vector endpoint diagrams as insets. Gray dashed lines show the vector difference sum (VDS) of the data, while black lines show the uncorrected, raw demagnetization data. Stereonets on the right show the directional evolution of the TRM during AF demagnetization. Natural remanent magnetization (NRM) directions for each specimen are shown in blue. Best fit great circles are shown for each specimen. Specimen MKA1-3D clearly shows a high-coercivity component that is oriented antiparallel to the applied field direction of the TRM. This self-reversed component is much reduced in specimen HHA3-2D, although is still detectable in the stereonet as the remanence direction begins to travel along a great circle containing the antiparallel direction. Specimen HH1-1C demonstrates a sample with no discernable antiparallel component.

behavior observed here. Instead, these Ti ratios are more likely to be intermediate composition titanohematite. Titanium ratios determined from microprobe analysis were accordingly plotted on the titanohematite solid-solution series in Figure 12, which suggest a possible range of titanohematite compositions from $y = 0.5–0.6$, consistent with observed Néel/Curie temperatures. SEM images using backscattered electrons

were collected from the same magnetic extracts used for EPMA analysis to check for potential microstructures within the Fe-Ti oxides. No evidence of intergrowths or other distinctive microstructural features were discerned and as such we do not include the images here.

6. Discussion

6.1. Magnetic Mineralogy of Hell Creek Sediments

Results from extensive rock magnetic analysis suggest that sediments from the Hell Creek region in Montana are composed of three principal magnetic minerals in various proportions: goethite, intermediate titanohematite, and magnetite/titanomagnetite (maghemite). Based on the results of the self-reversal tests, intermediate titanohematite is never so abundant so as to be the dominant (in the sense of intensity) remanence carrier, but does occur as a significant carrier of remanence (upward of 25%) in the majority of samples. The identification of the Verwey transition in low-temperature magnetometry experiments, persistent remanence above 400°C, and Curie temperatures ~580°C also support the presence of magnetite and titanomagnetite (or their partially oxidized equivalents) and suggest that these minerals are likely to be the primary holders of remanence. While the XRD results show the presence of titanomagnetite in only one sample, it is important to consider the coarse resolution of this nonmagnetic technique. Goethite is identified in select specimens in low-temperature magnetometry experiments, recognized by a large increase in remanence upon cooling and a wide spread between FC and ZFC curves for whole-rock samples.

The integration of information from our rock magnetic techniques and nonmagnetic techniques (similar to those used in past studies, e.g., *Force et al*. [2001]) lead us to conclude that the dominant magnetic carrier in our samples is magnetite/titanomagnetite(maghemite), while intermediate titanohematite is an important ancillary magnetic carrier phase in most samples. Calculated Néel/Curie temperatures of ~200°C are consistent with EPMA data and XRD results that suggest that the dominant mineralogy by mass is rhombohedral intermediate composition titanohematite, with compositions ranging from $y = 0.53–0.63$ (Figure 11). Furthermore, low-T magnetic experiments show a large magnitude increase in magnetization upon cooling for magnetic extracts, not due to goethite, which is suggestive of another mineral phase with low ordering temperature, but most likely intermediate titanohematite. The stronger saturation magnetization of magnetite and titanomagnetite, however, allow these minerals' remanence to overshadow that of titanohematite. Results from the self-reversal tests show evidence for a mineral phase that acquires a direction antiparallel to the applied field direction, consistent with the presence of intermediate titanohematite. These results are further corroborated with the moderate coercivities and saturating fields <300 mT observed in hysteresis measurements.

These mineralogic results, combined with evidence for SD grain sizes from FORC diagrams and the self-reversal test, suggest that the Hell Creek sediments have the capacity to be reliable paleomagnetic recorders over geologic time scales, provided that they have not been heated above ~200°C. Reheating of these sediments could result in a RTRM overprint, which would greatly complicate paleomagnetic interpretation. While goethite was likely formed during diagenesis after deposition, the intermediate titanohematite, magnetite, and titanomagnetite are likely primary detrital minerals in sediment derived from Laramide basement uplifts and Cretaceous volcanism to the west. Intermediate titanohematite only forms in limited geological environments (calc-alkaline volcanic centers), which is consistent with those associated with Cordilleran volcanism. This argument is further corroborated by the identification of intermediate titanohematite in Upper Cretaceous-lower Paleogene sediments in sedimentary basins throughout the central U.S. (Table 1 and Figure 1). Furthermore, intermediate titanohematite cannot form at near-surface conditions and therefore is unlikely to be due to diagenetic alteration. Thus, sediments from the Hell Creek region are likely to be reliable paleomagnetic recorders, given that the sediments have not been reheated above 200°C, or struck by lightning, and that care is taken to remove any remanence held by goethite.

6.2. Intermediate Titanohematite Recognition

We conclude that intermediate titanohematite is best recognized when observations from XRD and EPMA analysis, high-temperature susceptibility experiments, and the self-reversal test can be integrated. XRD and EPMA analysis along with high-temperature susceptibility measurements have been utilized before as means to identify the presence of intermediate titanohematite in the majority of previous studies [*Force et al*., 2001]. While these analyses are a reasonable means for identifying the presence of intermediate titanohematite, none of these experiments adequately tests whether this mineral phase is the primary carrier of remanence.

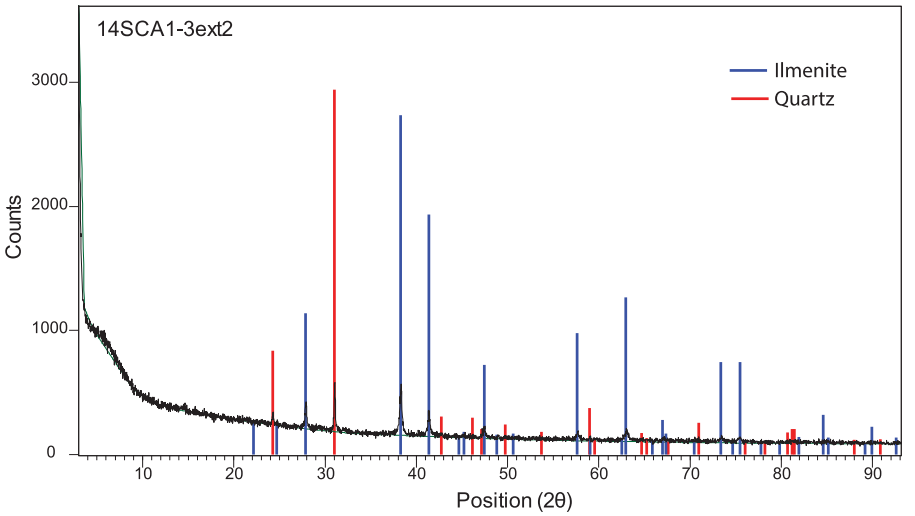

Figure 11. X-ray diffraction pattern for representative sample (14SCA1-3ext2). Colored lines mark spectra of mineral standards that were selected as best fits for the measured sample.

The self-reversal test, developed in this study, is a powerful new technique that not only provides a unique identifier of titanohematite (the presence of an antiparallel direction acquired at temperatures only slightly above blocking temperatures for intermediate titanohematite), but it also provides a good assessment of how much remanence is held by this phase. Furthermore, due to intermediate titanohematite's unique self-reversing property, this technique has the potential to stand on its own, unlike other analyses.

6.3. Comparison to Previous Studies

Comparing the results of this study to other rock magnetic and paleomagnetic studies on Late Cretaceous and Paleogene age clastic deposits across central North America, it can be seen that these sediments all share similar magnetic properties (Table 1). In all paleomagnetic studies, a primary signal was obtained between coercivities of 10 and 80 mT, and temperatures below 400°C, with calculated Curie temperatures ranging between 150 and 250°C. When conducted, XRD and EPMA analysis indicate the presence of intermediate composition titanohematite in all studies.

Of the selected studies shown in Table 1, intermediate titanohematite was identified or indicated in ~75% of these deposits extending in age from Late Cretaceous to Early Eocene. It is clear that due to similarities in magnetic properties, sediment source, and age, even in studies where titanohematite was not indicated as a primary magnetic recorder, it likely is present. However, overlaps in coercivity, unblocking temperatures, and Néel/Curie temperatures between intermediate titanohematite and magnetite/titanomagnetite (or their partially oxidized equivalents), along with common beliefs about the relative rarity of titanohematite in nature, create a situation where the potential presence of intermediate titanohematite is rapidly dismissed. Therefore, more advanced rock magnetic and nonmagnetic techniques are needed to test the importance of intermediate titanohematite to sedimentary remanence.

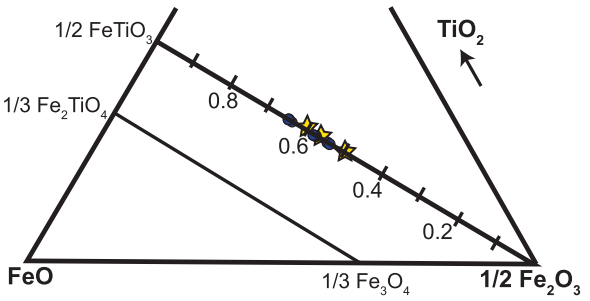

Figure 12. TiO_2-FeO-1/2Fe_2O_3 ternary diagram comparing titanohematite compositions determined from Néel/Curie temperatures (blue dots) and microprobe analysis of magnetic extracts (yellow stars). Calculated compositions from Néel/Curie temperature were determined using the calibration in *Moskowitz et al.* [2015].

Intermediate titanohematite has also been identified in economically important placer deposits that mark Upper Cretaceous shorelines extending from Montana to New Mexico [*Houston and Murphy*, 1962, 1977; *Force*, 2000; *Force et al.*, 2001] and in uranium-bearing Mesozoic and Cenozoic sandstones within central U.S. and south Texas [*Force et al.*, 2001]. Looking at the ages and distributions of these deposits in concert with those for the

intermediate titanohematite-bearing sediments discussed above, *Force et al.* [2001] suggest that the sources for this unique mineral come from three distinct volcanic centers of different age in three different areas within the U.S. This evidence suggests that geologic environments producing intermediate titanohematite are not as rare as they are presented in literature, and when these environments are coupled with effective sediment transport mechanisms, like those within the Late Cretaceous North American Cordillera, this mineral can become widespread in detrital deposits far beyond the volcanic source for millions of years. Therefore, it is likely that other sedimentary basins next to calc-alkaline volcanic centers, such as those in the Andes and other convergent margins, also preserve intermediate titanohematite, even if RTRMs are not preserved in outcropping volcanics. Understanding the role intermediate titanohematite plays in sedimentary remanence is imperative for proper paleomagnetic interpretation as intermediate titanohematite, due to its low unblocking temperatures combined with its ability to acquire a RTRM, has the potential to complicate paleomagnetic records. While the current literature suggests that intermediate titanohematite is rare in nature, it appears that more specialized yet straightforward rock magnetic analysis may reveal it to be more abundant in the rock record than previously thought.

7. Conclusion

Extensive rock magnetic analyses on sediments that span the Cretaceous-Paleogene boundary in the Hell Creek region, Montana show that the dominant ferrimagnetic mineral by mass is intermediate composition titanohematite with compositions ranging from $y = 0.53–0.63$. The dominant magnetic remanence carrier, however, is probably magnetite and titanomagnetite(maghemite). Néel/Curie temperature determination and XRD and EPMA analysis are effective techniques for recognizing the presence of intermediate titanohematite. The self-reversal test, a new technique developed in this study for intermediate titanohematite identification, contributes information about how much of a sediment's remanence may (or may not) be held by intermediate titanohematite. Further development, however, is needed to make it into a tool that is capable of detecting a greater range of titanohematite compositions. The similar magnetic properties shared between our sediments and coeval sediments across the central U.S. suggest that titanohematite may carry a greater fraction of natural remanent magnetization than previously recognized, which is important to characterize in order to avoid biased paleomagnetic interpretation. Although geologic environments where intermediate composition titanohematite forms are limited, if they are coupled with efficient sediment transport mechanisms, then this mineral can become widespread in detrital sediment deposits over millions of years of deposition. It is likely that other sedimentary basins sourced from intermediate calc-alkaline volcanic centers also preserve intermediate titanohematite and that this mineral may be more abundant in the rock record than previously perceived.

Acknowledgments

We thank the Institute for Rock Magnetism (IRM), the Geological Society of America, and the Esper S. Larsen Fund for support of this work. Sample analysis was funded by an IRM visiting fellowship awarded to the first author. The first author was further funded by the National Science Foundation Graduate Research Fellowship. We further thank Tim Teague and Sean Mulcahy (now at Western Washington University) at the University of California Berkeley for help with XRD analysis, SEM imaging, and EPMA analysis. We would also like to thank the entire IRM staff for their overwhelming support and kindness during the first author's brief visit, and especially Bruce Moskowitz who brilliantly suggested we try a self-reversal test. We'd also like to thank reviewers Pete Lippert and Rob Coe for their positive reviews and constructive comments that helped improve this manuscript. The data presented in the paper can be found in the MagIC database.

References

Archibald, J. D., R. F. Butler, E. H. Lindsay, W. A. Clemens, and L. Dingus (1982), Upper Cretaceous-Paleocene biostratigraphy and magnetostratigraphy, Hell Creek and Tullock Formations, northeastern Montana, *Geology*, *10*, 153–159, doi:10.1130/0091-7613(1982)10 < 153:UCBAMH>2.0.CO;2.

Bilardello, D., and M. Jackson (2013), What do the Mumpsies do?, *IRM Q.*, *23*(3), 11–15.

Bina, M., J. C. Tanguy, V. Hoffmann, M. Prévot, E. L. Listanco, R. Keller, K. Th. Fehr, A. T. Goguitchaichvili, and R. S. Punongbayan (1999), A detailed magnetic and mineralogical study of self-reversed dacitic pumices from the 1991 Pinatubo eruption (Philippines), *Geophys. J. Int.*, *138*, 159–178.

Boyd, D. W., and J. A. Lillegraven (2011), Persistence of the Western Interior Seaway Historical background and significance of ichnogenus Rhizocorallium in Paleocene strata, south-central Wyoming, *Rocky Mt. Geol.*, *46*, 43–69, doi:10.2113/gsrocky.46.1.43.

Burton, B. P., P. Robinson, S. A. McEnroe, K. Fabian, and T. B. Ballaran (2008), A low-temperature phase diagram for ilmenite-rich compositions in the system Fe_2O_3-$FeTiO_3$, *Am. Mineral.*, *93*(8–9), 1260–1272.

Butler, R. (1982), Magnetic mineralogy of continental deposits, San Juan Basin, New Mexico, and Clark's Fork Basin, Wyoming, *J. Geophys. Res.*, *87*(B9), 7843–7852, doi:10.1029/JB087iB09p07843.

Butler, R. F., and E. H. Lindsay (1985), Mineralogy of magnetic minerals and revised magnetic polarity stratigraphy of continental sediments, San Juan Basin, New Mexico, *J. Geol.*, *93*, 535–554.

Butler, R. F., P. D. Gingerich, and E. H. Lindsay (1981), Magnetic polarity stratigraphy and biostratigraphy of Paleocene and Lower Eocene continental deposits, Clark's Fork Basin, Wyoming, *J. Geol.*, *89*, 299–316.

Butler, R. F., D. W. Krause, and P. D. Gingerich (1987), Magnetic polarity stratigraphy and biostratigraphy of Middle-Late Paleocene continental deposits of South-Central Montana, *J. Geol.*, *95*, 647–657.

Cherven, V. B., and A. F. Jacob (1985), Evolution of Paleogene depositional systems, Williston Basin, in response to global sea level changes, in *Cenozoic Paleogeography of the West-Central United States: Society of Economic Paleontologists and Mineralogists, Rocky Mountain Section*, edited by R. M. Flores and S. S. Kaplan, pp. 127–170, The Rocky Mountain Section, Society of Economic Paleontologists and Mineralogists, Denver, Colo.

Church, N., J. Feinberg, and R. Harrison (2011), Low-temperature domain wall pinning in titanomagnetite: Quantitative modeling of multidomain first-order reversal curve diagrams and AC susceptibility, *Geochem. Geophys. Geosyst.*, *12*, Q07Z27, doi:10.1029/2011GC003538.

Cox, A., R. R. Doell, and G. B. Dalrymple (1963), Geomagnetic polarity epochs and Pleistocene geochronometry, *Nature*, *198*, 1049–1051, doi:10.1038/1981049a0.
Day, R., M. Fuller, and V. A. Schmidt (1977), Hysteresis properties of titanomagnetites: Grain-size and compositional dependence, *Phys. Earth Planet. Inter.*, *13*, 260–267.
Dekkers, M. J. (1989), Magnetic properties of natural goethite—II. TRM behaviour during thermal and alternating field demagnetization and low-temperature treatment, *Geophys. J.*, *97*, 341–355.
Diehl, J. F. (1991), The Elkhorn Mountains revisited: New data for the Late Cretaceous paleomagnetic field of North America, *J. Geophys. Res.*, *96*(B6), 9887–9894, doi:10.1029/91JB00959.
Dunlop, D. J. (2002), Theory and application of the Day plot (Mrs/Ms versus Hcr/Hc): 1. Theoretical curves and tests using titanomagnetite data, *J. Geophys. Res.*, *107*(B3), doi:10.1029/2001JB000486.
Dunlop, D. J., and Ö. Özdemir (1997), *Rock Magnetism: Fundamentals and Frontiers*, 573 pp., Cambridge Univ. Press, Cambridge, U. K.
Egli, R. (2013), VARIFORC: An optimized protocol for calculating non-regular first-order reversal curve (FORC) diagrams, *Global Planet. Change*, *110*, 302–320.
Fabian, K., N. Miyajima, P. Robinson, S. A. McEnroe, T. B. Ballaran, and B. P. Burton (2011), Chemical and magnetic properties of rapidly cooled metastable ferri-ilmenite solid solutions: Implications for magnetic self-reversal and exchange bias—I. Fe-Ti order transition in quenched synthetic ilmenite 61, *Geophys. J. Int.*, *186*, 997–1014, doi:10.1111/j.1365-246X.2011.05109.x.
Fabian, K., V. P. Shcherbakov, and S. A. McEnroe (2013), Measuring the Curie temperature, *Geochem. Geophys. Geosyst.*, *14*, 947–961, doi:10.1029/2012GC004440.
Fastovsky, D. E. (1987), Paleoenvironments of vertebrate bearing strata during the Cretaceous-Paleogene transition, eastern Montana and western North Dakota, *Palaios*, *2*, 282–295, doi:10.2307/3514678.
Force, E. R. (2000), Titanium-mineral resources of the western U.S.—An update, *U.S. Geol. Surv. Open File Rep., OF 00-442*, 43 pp.
Force, E. R., R. F. Butler, R. L. Reynolds, and R. S. Houston (2001), Magnetic ilmenite-hematite detritus in Mesozoic-Tertiary Placer and sandstone-hosted uranium deposits of the Rocky Mountains, *Econ. Geol.*, *96*, 1445–1453, doi:10.2113/gsecongeo.96.6.1445.
France, D. E., and F. Oldfield (2000), Identifying goethite and hematite from rock magnetic measurements of soils and sediments, *J. Geophys. Res.*, *105*(B2), 2781–2795.
Gill, J. R., and W. A. Cobban (1973), Stratigraphy and geologic history of the Montana Group and equivalent rocks, Montana, Wyoming, and North and South Dakota, *U.S. Geol. Surv. Prof. Pap.*, *776*, 36 pp.
Goguitchaichvili, A., and M. Prévot (2000), Magnetism of oriented single crystals of hemolilmenite with self-reversed thermoremanent magnetization, *J. Geophys. Res.*, *105*(B2), 2761–2780.
Haag, M., F. Heller, J. C. Carracedo, and V. Soler (1990a), Remanent magnetization of andesitic and dacitic pumice from the 1985 eruption of Nevado del Ruiz (Colombia) reversed due to self-reversal, *J. Volcanol. Geotherm. Res.*, *41*, 369–377, doi:10.1016/0377-0273(90)90097-Y.
Haag, M., F. Heller, R. Allenspach, and K. Roch (1990b), Self-reversal of natural remanent magnetization n andesitic pumic, *Phys. Earth Planet. Inter.*, *65*(1), 104–108.
Haag, M., F. Heller, M. Lutz, and E. Reusser (1993), Domain observations of the magnetic phases in volcanics with self-reversed magnetization, *Geophys. Res. Lett.*, *20*, 675–678.
Harrison, R. J., and J. M. Feinberg (2008), FORCinel: An improved algorithm for calculating first-order reversal curve distributions using locally weighted regression smoothing, *Geochem. Geophys. Geosyst.*, *9*, Q05016, doi:10.1029/2008GC001987.
Hartman, J. H. (2002), Hell Creek Formation and the early picking of the Cretaceous-Tertiary boundary in the Williston Basin, in *The Hell Creek Formation and the Cretaceous-Tertiary Boundary in the Northern Great Plains: An Integrated Continental Record of the End of the Cretaceous*, edited by J. H. Hartman, K. R. Johnson, and D. J. Nichols, *Spec. Pap. Geol. Soc. Am., 361*, 1–7, doi:10.1130/0-8137-2361-2.1.
Hartman, J. H., R. D. Butler, M. W. Weiler, and K. K. Schumaker (2014), Context, naming, and formal designation of the Cretaceous Hell Creek Formation lectostratotype, Garfield County, Montana, in *Through the End of the Cretaceous in the Type Locality of the Hell Creek Formation in Montana and Adjacent Areas*, edited by G. P. Wilson et al., *Spec. Pap. Geol. Soc. Am., 503*, 1–34.
Heller, F., J. C. Carracedo, and V. Solert (1986), Reversed magnetization in pyroclastics from the 1985 eruption of Nevado del Ruiz, Colombia, *Nature*, *324*, 241–242, doi:10.1038/324241a0.
Hoffman, K. A. (1975), Cation diffusion processes and self-reversal of thermoremanent magnetization in the ilmenite-haematite solid solution series, *Geophys. J. Int.*, *41*, 65–80, doi:10.1111/j.1365-246X.1975.tb05485.x.
Hoffman, K. A. (1992), Self-reversal of thermoremanent magnetization in the ilmenite-hematite system- Order-disorder, symmetry, and spin alignment, *J. Geophys. Res.*, *97*(B7), 10,833–10,895.
Hoffmann, V., and K. T. Fehr (1996), Micromagnetic, rock magnetic and mineralogical studies on Dacitic Pumice from the Pinatubo Eruption (1991, Phillipines) Showing self-reversed TRM, *Geophys. Res. Lett.*, *23*(20), 2835–2838, doi:10.1029/96GL01317.
Houston, R. S., and J. F. Murphy (1962), Titaniferous black sandstone deposits of Wyoming, *Geol. Soc. Wyoming Bull.*, *49*, 120.
Houston, R. S., and J. F. Murphy (1977), Depositional environment of Upper Cretaceous black sandstones of the western interior, U.S. Geol. Surv. Prof. Pap. 994A, 29 pp.
Ishikawa, Y. (1962), Magnetic properties of ilmenite-hematite system at low temperature, *J. Phys. Soc. Jpn.*, *17*, 1835–1843, doi:10.1143/JPSJ.17.1835.
Ishikawa, Y., and S. Akimoto (1957), Magnetic properties of the $FeTiO_3$-Fe_2O_3 solid solution series, *J. Phys. Soc. Jpn.*, *12*, 1083–1098, doi:10.1143/JPSJ.12.1083.
Ishikawa, Y., and Y. Syono (1962), Reverse thermo-remanent magnetism in $FeTiO_3$-Fe_2O_3 system, *J. Phys. Soc. Jpn.*, *17*, 714–718.
Ishikawa, Y., and Y. Syono (1963), Order-disorder transformation and reverse thermo-remanent magnetism in the $FeTiO_3$-Fe_2O_3 system, *J. Phys. Chem. Solids*, *24*, 517–528.
Kennedy, L. P. (1981), Self-reversed thermoremanent magnetization in a Late Brunhes Dacite Pumice, *J. Geomagn. Geoelectr.*, *33*, 429–448, doi:10.5636/jgg.33.429.
Kennedy, L. P., and M. D. Osborne (1987), Composite titanomagnetite-ferrian ilmenite grains and correlative magnetic components in a dacite with self-reversed TRM, *Earth Planet. Sci. Lett.*, *84*, 479–486, doi:10.1016/0012-821X(87)90012-4.
Krása, D., V. P. Shcherbakov, T. Kunzmann, and N. Petersen (2005), Self-reversal of remanent magnetization in basalts due to partially oxidized titanomagnetites, *Geophys. J. Int.*, *162*(1), 115–136.
Lagroix, F., S. K. Banerjee, and B. M. Moskowitz (2004), Revisiting the mechanism of reversed thermoremanent magnetization (rTRM) based on observations from synthetic titanohematite (y = 0.7), *J. Geophys. Res.*, *109*, B12108, doi:10.1029/JB003076.
Lawson, C. A., G. L. Nord Jr., and D. E. Champion (1987), Fe-Ti oxide mineralogy and the origin of normal and reverse remanent magnetization in dacitic pumice blocks from Mt. Shasta, California, *Phys. Earth Planet. Inter.*, *46*, 270–288, doi:10.1016/0031-9201(87)90190-7.

LeCain, R., W. C. Clyde, G. P. Wilson, and J. Riedel (2014), Magnetostratigraphy of the Hell Creek and lower Fort Union Formations in northeastern Montana, *Spec. Pap. Geol. Soc. Am.*, *503*, 137–147, doi:10.1130/2014.2503(04).

Lerbekmo, J. F. (1999), Magnetostratigraphy of the Canadian continental drilling program Cretaceous-Tertiary (K-T) boundary project core holes, western Canada, *Can. J. Earth Sci.*, *36*, 705–715, doi:10.1139/e98-066.

Lerbekmo, J. F., and K. C. Coulter (1984), Magnetostratigraphic and biostratigraphic correlations of Late Cretaceous to Early Paleocene Strata between Alberta and North Dakota, in *The Mesozoic of Middle North America, Can. Soc. Pet. Geol. Mem.*, vol. 9, edited by D. F. Stott and D. J. Glass, pp. 313–317, Canadian Society for Petroleum Geologists, Calgary, Alberta, Canada.

Lerbekmo, J. F., and K. C. Coulter (1985), Magnetostratigraphic and lithostratigraphic correlation of coal seams and Contiguous Strata, Upper Horseshoe Canyon and Scollard Formations (Maastrichtian to Paleocene), Red Deer Valley, Albertam, *Bull. Can. Pet. Geol.*, *33*, 295–305.

Lindsay, E. H., R. F. Butler, and N. M. Johnson (1981), Magnetic polarity zonation and biostratigraphy of late Cretaceous and Paleocene continental deposits, San Juan Basin, New Mexico, *Am. J. Sci.*, *281*, 390–435.

Lowrie, W. (1990), Identification of ferromagnetic minerals in a rock by coercivity and unblocking temperature properties, *Geophys. Res. Lett.*, *17*(2), 159–162, doi:10.1029/GL017i002p00159.

Lowrie, W., and F. Heller (1982), Magnetic properties of marine limestones, *Rev. Geophys.*, *20*, 171–192.

Lund, S. P., J. H. Hartman, and S. K. Banerjee (2002), Magnetostratigraphy of interfingering Upper Cretaceous-Paleocene marine and continental strata of the Williston Basin, North Dakota and Montana: The Hell Creek Formation and the Cretaceous-Tertiary Boundary in the northern Great Plains, *Spec. Pap. Geol. Soc. Am.*, *361*, 57–74.

McDougall, I., and D. H. Tarling (1963), Dating of reversals of the earth's magnetic field, *Nature*, *198*, 1012–1013.

Moskowitz, B. M., M. Jackson, and C. Kissel (1998), Low-temperature magnetic behavior of titanomagnetites, *Earth Planet. Sci. Lett.*, *157*(3–4), 141–149.

Moskowitz, B. M., M. Jackson, and V. Chandler (2015), Geophysical properties of the near-surface Earth: Magnetic properties, in *Treatise on Geophysics*, 2nd ed., edited by G. Schubert, chap. 11.05, pp. 139–174, Elsevier, Oxford, U. K., doi:10.1016/B978-0-444-53802-4.00191-3.

Nagata, T. (1961), *Rock Magnetism*, 366 pp., Maruzen Co., Tokyo.

Nagata, T., and S. Akimoto (1956), Magnetic properties of ferromagnetic ilmenites, *Geofis. Pura Appl.*, *34*, 36–50, doi:10.1007/BF02122815.

Nagata, T., and S. Uyeda (1959), Exchange interaction as a cause of reverse thermo-remanent magnetism, *Nature*, *184*, 890–891, doi:10.1038/184890a0.

Nagata, T., S. Akimoto, and S. Uyeda (1951), Reverse thermo-remanent magnetism, *Proc. Jpn. Acad.*, *27*, 643–645, doi:10.2183/pjab1945.27.643.

Nord, G. L., and C. A. Lawson (1989), Order-disorder transition-induced twin domains and magnetic properties in ilmenite-hematite, *Am. Mineral.*, *74*, 160–176.

Ozima, M., and M. Funaki (2001), Magnetic properties of hemoilmenite single crystals in Haruna dacite pumice revealed by the Bitter technique, with special reference to self-reversal of thermoremanent magnetization, *Earth Planets Space*, *53*, 111–119, doi:10.1186/BF03352368.

Ozima, M., M. Funaki, N. Hamada, S. Aramaki, and T. Fujii (1992), Self-reversal of thermo-remanent magnetization in pyroclastics from the 1991 eruption of Mt. Pinatubo, Philippines, *J. Geomagn. Geoelectr.*, *44*, 979–984, doi:10.5636/jgg.44.979.

Ozima, M., O. Oshima, and M. Funaki (2003), Magnetic properties of pyroclastic rocks from the later stage of the eruptive activity of Haruna Volcano in relation to the self-reversal of thermo-remanent magnetization, *Earth Planets Space*, *55*, 183–188, doi:10.1186/BF03351747.

Peppe, D. J., D. A. D. Evans, and A. V. Smirnov (2009), Magnetostratigraphy of the Ludlow Member of the Fort Union Formation (Lower Paleocene) in the Williston Basin, North Dakota, *Geol. Soc. Am. Bull.*, *121*, 65–79, doi:10.1130/B26353.1.

Peppe, D. J., K. R. Johnson, and D. A. D. Evans (2011), Magnetostratigraphy of the Lebo and Tongue River Members of the Fort Union Formation (Paleocene) in the northeastern Powder River Basin, Montana, *Am. J. Sci.*, *311*, 813–850, doi:10.2475/10.2011.01.

Renne, P. R., A. L. Deino, F. J. Hilgen, K. F. Kuiper, D. F. Mark, W. S. Mitchell III, L. E. Morgan, R. Mundil, and J. Smit (2013), Time scales of critical events around the Cretaceous-Paleogene boundary, *Science*, *339*, 684–687, doi:10.1126/science.1230492.

Robinson, P., R. J. Harrison, N. Miyajima, S. A. McEnroe, and K. Fabian (2012a), Chemical and magnetic properties of rapidly cooled metastable ferri-ilmenite solid solutions: Implications for magnetic self-reversal and exchange bias—II. Chemical changes during quench and annealing, *Geophys. J. Int.*, *188*, 447–472, doi:10.1111/j.1365-246X.2011.05277.x.

Robinson, P., R. J. Harrison, K. Fabian, and S. A. McEnroe (2012b), Chemical and magnetic properties of rapidly cooled metastable ferri-ilmenite solid solutions: Implications for magnetic self-reversal and exchange bias—III: Magnetic interactions in samples produced by Fe-Ti ordering, *Geophys. J. Int.*, *191*, 1025–1047, doi:10.1111/j.1365-246X.2012.05692.x.

Robinson, P., S. A. McEnroe, K. Fabian, R. J. Harrison, C. I. Thomas, and H. Mukai (2014), Chemical and magnetic properties of rapidly cooled metastable ferri-ilmenite solid solutions—IV: The fine structure of self-reversed thermoremanent magnetization, *Geophys. J. Int.*, *196*, 1375–1396, doi:10.1093/gji/ggt486.

Sprain, C. J., P. R. Renne, G. P. Wilson, and W. A. Clemens (2015), High-resolution chronostratigraphy of the terrestrial Cretaceous-Paleogene transition and recovery interval in the Hell Creek, region, Montana, *Geol. Soc. Am. Bull.*, *127*(3–4), 393–409.

Strehlau, J. H., L. A. Hegner, B. E. Strauss, J. M. Feinberg, and R. L. Penn (2014), Simple and efficient separation of magnetic minerals from speleothems and other carbonates, *J. Sediment. Res.*, *84*, 1096–1106.

Swisher, C. C., III, L. Dingus, and R. F. Butler (1993), 40Ar/39Ar dating and magnetostratigraphic correlation of the terrestrial Cretaceous-Paleogene boundary and Puercan Mammal Age, Hell Creek—Tullock formations, eastern Montana, *Can. J. Earth Sci.*, *30*, 1981–1996, doi:10.1139/e93-174.

Taylor, L. H., and R. F. Butler (1980), Magnetic-polarity stratigraphy of Torrejonian sediments, Nacimiento Formation, San Juan Basin, New Mexico, *Am. J. Sci.*, *280*, 97–115, doi:10.2475/ajs.280.2.97.

Uyeda, S. (1957), Thermo-remanent magnetism and coercive force of the ilmenite-hematite series, *J. Geomagn. Geoelectr.*, *9*, 61–78, doi:10.5636/jgg.9.61.

Uyeda, S. (1958), Thermo-remanent magnetism as a medium of paleomagnetism, with special reference to reverse thermo-remanent magnetism, *Jpn. J. Geophys.*, *2*, 1–123.

Wang, D., and R. Van der Voo (2004), The hysteresis properties of multidomain magnetite and titanomagnetite/titanomaghemite in mid-ocean ridge basalts, *Earth Planet. Sci. Lett.*, *220*, 175–184.